AD-A226 223

ATION PAGE

Form Approved
OMB No. 0704-0188

(Leave blank)	2. REPORT DATE	3. REPORT TYPE AND DATES COVERED
	July 1990	Technical

4. TITLE AND SUBTITLE
Infrared and Microwave Dielectric Relaxation of Benzonitrile, Acetonitrile and Their Mixtures with Carbon Tetrachloride at 25degC

5. FUNDING NUMBERS
DAALO3-89-K-0148

6. AUTHOR(S)
A. Marchetti, Xu Meizhen, Edward M. Eyring
Sergio Petrucci

7. PERFORMING ORGANIZATION NAME(S) AND ADDRESS(ES)
Polytechnic Univ of Farmingdale
Farmingdale, NY 11735

DTIC
ELECTE
AUG 30 1990
S D

8. PERFORMING ORGANIZATION REPORT NUMBER

9. SPONSORING/MONITORING AGENCY NAME(S) AND ADDRESS(ES)
U. S. Army Research Office
P. O. Box 12211
Research Triangle Park, NC 27709-2211

10. SPONSORING/MONITORING AGENCY REPORT NUMBER
ARO 26636.1-CH

11. SUPPLEMENTARY NOTES
The view, opinions and/or findings contained in this report are those of the author(s) and should not be construed as an official Department of the Army position, policy, or decision, unless so designated by other documentation.

12a. DISTRIBUTION/AVAILABILITY STATEMENT
Approved for public release; distribution unlimited.

12b. DISTRIBUTION CODE

13. ABSTRACT *(Maximum 200 words)*

Infrared refractive indices at $\bar{\nu} \simeq 300$ cm^{-1} (f = 9000 GHz) and $\bar{\nu} \simeq 400$ cm^{-1} (f = 12,000 GHz) and complex permittivities, $\epsilon^* = \epsilon' - J\epsilon''$ at $\bar{\nu} \simeq 300$ cm^{-1} and $\bar{\nu} \simeq 400$ cm^{-1} for acetonitrile and acetonitrile-carbon tetrachloride as well as benzonitrile and benzonitrile-carbon tetrachloride mixtures at 25°C are reported. Microwave complex permittivities, ϵ^*, in the frequency range ~0.4 to 90 GHz for the same systems at 25°C, are also reported. The microwave

(Cont'd on reverse side)

14. SUBJECT TERMS
Infrared Refractive Indices, Benzonitriles, Acetonitrile, Carbon Tetrachloride

15. NUMBER OF PAGES

16. PRICE CODE

17. SECURITY CLASSIFICATION OF REPORT	18. SECURITY CLASSIFICATION OF THIS PAGE	19. SECURITY CLASSIFICATION OF ABSTRACT	20. LIMITATION OF ABSTRACT
UNCLASSIFIED	UNCLASSIFIED	UNCLASSIFIED	UL

results extend literature data previous imited to f < 18 GHz, for pure acetonitrile and to f < 36 GHz, for benzonitrile. The infrared refractive indices at $\bar{\nu} \approx 300$ cm^{-1} substitute for previously reported literature values at $\bar{\nu} \approx 200$ cm^{-1}, judged to be of inadequate precision.

Infrared and Microwave Dielectric Relaxation of Benzonitrile, Acetonitrile and Their Mixtures with Carbon Tetrachloride at 25°C

A. Marchetti†, Meizhen, Xu, Edward M. Eyring and Sergio Petrucci*
Weber Research Institute, Polytechnic
University of Farmingdale, NY 11735, and
Department of Chemistry, University of Utah
Salt Lake City, UT 84112

†On leave of absence from the University of Modena, Modena, Italy

Abstract

Infrared refractive indices at $\bar{\nu} \simeq 300$ cm^{-1} (f = 9000 GHz) and $\bar{\nu} \simeq 400$ cm^{-1} (f = 12,000 GHz) and complex permittivities $\epsilon^* = \epsilon' - J\epsilon''$ at $\bar{\nu} \simeq 300$ cm^{-1} and $\bar{\nu} \simeq 400$ cm^{-1} for acetonitrile and acetonitrile-carbon tetrachloride as well as benzonitrile and benzonitrile-carbon tetrachloride mixtures at 25°C are reported. Microwave complex permittivities ϵ^*, in the frequency range ~0.4 to 90 GHz for the same systems at 25°C, are also reported. The microwave results extend literature data previously limited to f < 18 GHz for pure acetonitrile and to f < 36 GHz for benzonitrile. The infrared refractive indices at $\bar{\nu} \simeq 300$ cm^{-1} substitute for previously reported literature values at $\bar{\nu} \simeq 200$ cm^{-1}, judged to be of inadequate precision. The observed relaxation processes for pure benzonitrile and acetonitrile can be described either by a single Debye relaxation function, using a parameter ϵ_∞, or by a Cole-Davidson distribution function using the squared IR refractive index n_{IR}^2 at $\bar{\nu} \simeq 300$ cm^{-1}. The significance of these alternatives is discussed. This study has theoretical relevance when related to the need for knowledge of ϵ_∞ (or n_{IR}^2) in evaluating the longitudinal relaxation times τ_L and the short range structural relaxation time τ_G in femtosecond-picosecond molecular dynamics studies of solvation. A more practical application of the present work in liquid mixtures is the need for molecular information on the relations

between chemical structure and dielectric properties of liquids to be used in supercapacitors. Visible refractive indices at λ = 589.3 nm, the sodium D line, for benzonitrile and benzonitrile-carbon tetrachloride mixtures, for acetonitrile and acetonitrile-carbon tetrachloride mixtures are also reported. Static dielectric permittivities for benzonitrile, acetonitrile and their mixtures with carbon tetrachloride at 25°C are reported, confirming the extrapolated ϵ_o values from microwave data. The results of the present work encompass all the spectral range from 1 MHz to 16,969 cm^{-1} (f = 509 THz) namely the sodium doublet line in the visible.

Introduction

Microwave techniques for determining the complex permittivity $\epsilon^* = \epsilon' - J\epsilon''$ of liquids and liquid mixtures have been developed mainly since World War II with results reported in monographs.[1]

It has been evident since at least 1955, as reported by Poley,[2] that the Debye theory of a single relaxation process (for the decay of the polarization) gives reasonable fits to ϵ' vs frequency data, only up to frequencies of ~40 GHz. Above 60-70 GHz, for many liquids such as chlorobenzene,[3] tails of the main relaxation process appear.

Moreover, it has been shown that the value of ϵ_∞ (the extrapolated figure for ϵ' at frequencies high with respect to the Debye relaxation frequency f_r) is generally larger than n_{IR}^2, and larger than n_D^2 the squared far-infrared refractive index at λ = 589.3 nm, corresponding to the Na-doublet in the visible. In fact, for water n^2 goes from 4.55 at 30 cm^{-1} [4] corresponding to ϵ_∞ extrapolated from microwave data to n_{IR}^2 = 1.76 at 400 cm^{-1} which is close to n_D^2 = 1.777 (at 16,969 cm^{-1}).[4]

For rigid molecular liquids such as C_6H_5-X, Hill[5] proposed a libration resonant-relaxation theory which would add to the rotational Debye process a new type of process (a partial rotation between neighbor potential wells) distinct from the Debye full rotational one. Also, first Lorentz,[6] and later Van Vleck and Weisskopf[7] proposed a theory of damped resonant absorptions for the atomic and electronic polarizations that would affect the permittivity n^2 at infrared (IR) and optical frequencies. These processes would lead to the progressive decay of the atomic polarization at IR frequencies and to the electronic polarization at visible and UV frequencies.

The numerical interpretation of the dielectric spectra requires a knowledge of ϵ_∞ and/or of n^2_{IR} to be used and further requires adequate theoretical criteria for the choice. As recently as 1989, it was remarked that the understanding of this region of the dielectric spectra of liquids is limited.[8]

In addition, a knowledge of the numerical value of ϵ_∞ for liquids is essential to calculations of both the solvent rearrangement times of a liquid around a solute (either τ_L, the long range longitudinal relaxation time, or τ_G, the short range structural relaxation time)[9] explored by femtosecond-picosecond spectroscopy. With these goals in mind we have started a research program to provide reliable experimental $\epsilon^* = \epsilon' - j\epsilon''$ data at both microwave and infrared frequencies in liquids.

Benzonitrile[2] and acetonitrile[10] were studied in the past in a limited frequency range. Unfortunately, for acetonitrile-carbon tetrachloride mixtures infrared refractive indices of inadequate precision were reported.[10] We decided to start from these systems trying to present data of adequate range above 36 GHz for benzonitrile[2] and above 18 GHz for acetonitrile.[10]

Mixtures of acetonitrile and benzonitrile have also been investigated, as they give clues to the self association of the polar component of the mixture. For CH_3CN the self association phenomenon has already been studied quantitatively by NMR techniques.[11]

Also adequate data for refractive indices at $\bar{\nu} \simeq 300$ cm^{-1} (f = 9000 GHz and $\bar{\nu} \simeq 400$ cm^{-1} (f = 12,000 GHz)) are reported. Static dielectric permittivities ϵ_o for the two solvents and their mixtures with CCl_4 are also reported at 25°C.

Development of a high charge storage capacitor for high frequency circuitry has been advocated.[12] Such capacitors require liquids and liquid mixtures of relatively high permittivity to fill the capacitor and to hold the charge. Thus mixtures of apolar-polar components are needed for which there is adequate knowledge of their dielectric properties and of the relations between chemical structure of the polar component and the dielectric properties. The present study is the first step in this direction.

Experimental

The refractive indices at infrared frequencies of about 300 cm^{-1} have been determined by scanning the frequency between 180 and ~400 cm^{-1} with a dispersive Perkin-Elmer 983 G spectrometer, computer assisted for digitizing and recording of transmittances. A 0.1 mm optical path length, silicon windowed, sealed, 1400 series cell (provided by Specac, U.K. and distributed by NSG Precision Cells Inc., Farmingdale, NY who sealed the windows) was used. The refractive indices at ~400 cm^{-1} were determined by scanning the same instrument between 300 cm^{-1} and 500 cm^{-1} but using a sealed Perkin-Elmer cell (0.1 mm optical path) with KRS5 windows. The sealed cells were thermostatted

at 25.0°C by liquid circulating in a jacket holding the cell. The temperature was monitored by a thermistor attached to the sample cell jacket, and the thermostat was regulated by a proportional thermoregulator with a sensitivity of 10^{-2}°C.

The frequency was scanned with the cell first empty and then filled with the liquid under study in a double beam mode. A minimum of 15 minutes was required for the cell to acquire mechanical stability with temperature, even when empty. This was determined by scanning at various times and determining the empty cell thickness by the fringe method. Only after about 15 minutes did the cell thickness remain constant.

The fringe method was then used with the cell filled with the thermostatted liquid under study after thermal equilibration. Fringes were digitized and recorded by the spectrometer and the apparent length of the cell empty, ℓ_o, and full, ℓ, were calculated by linear regression of "peak" wave number vs peak number.

Representative plots of the record "peaks" for both the empty cell and the cell filled with acetonitrile are reported in Figs. 1A and 1B. The refractive index is the ratio (see Appendix)

$$n = \ell/\ell_o \qquad (1)$$

and is the average value at $\bar{\nu} \simeq 300$ cm^{-1} for the 180-400 cm^{-1} range and at $\bar{\nu} \simeq 400$ cm^{-1} for the 300-500 cm^{-1} range. The peak at $\bar{\nu} \simeq 378$ cm^{-1} is one of the resonance bands of acetonitrile or benzonitrile, and it has been, of course, avoided in the "peak" counting by the fringe method.

For the attenuation constant α (neper cm^{-1}), a variable path cell (Janos,Townsend,VT) with a minimum fiduciary mark division of 5 micrometers and KRS5 windows has been used at $\bar{\nu} \simeq 300$ cm^{-1}. Some measurements were

performed with a variable path cell (Specac, U.K.) with minimum fiduciary mark divisions of 5 micrometers and silicon windows. The absorbance A vs path length increment $\Delta\ell$ was recorded. Figure 2 reports one of the plots of A vs $\Delta\ell$ (with 0 marked as the beginning of the values read) for acetonitrile at 25°C and $\bar{\nu} \simeq 300$ cm^{-1} (f = 9000 GHz).

We recall that

$$A = \log_{10} \frac{1}{T} = \log_{10} \frac{P_o}{P} \tag{2}$$

where T is the transmittance and P_o and P are the power at distances 0 and ℓ, respectively. Further, because of the Lambert-Beer law

$$I = I_o e^{-\alpha\ell} \ , \ P = P_o e^{-2\alpha\ell} \tag{3}$$

with $I^2 = P$, the squared intensity equal to the power, and

$$\alpha = \frac{2.30103}{2} \ \frac{A}{\ell} \tag{4}$$

Therefore a plot of A vs ℓ at the wavenumber $\bar{\nu}$, as depicted in Fig. 2, gives α from the slope of the plot. The wavelength λ is calculated from $n = \frac{\lambda_o}{\lambda}$ hence ϵ' and ϵ'' can be calculated from the relations

$$\epsilon' = \left(\frac{\lambda_o}{\lambda}\right)^2 \left[1 - \left(\frac{\alpha\lambda}{2\pi}\right)^2\right]$$
$$\epsilon'' = \left(\frac{\lambda_o}{\lambda}\right)^2 \frac{\alpha\lambda}{\pi} \tag{5}$$

Here λ_o denotes the free space wavelength.

Numerically for the present systems at $\bar{\nu} \simeq 300$ cm^{-1}, $\epsilon' = n^2$ within experimental error as the term $\left[1 - \left(\frac{\alpha\lambda}{2\pi}\right)^2\right]$ is practically equal to one. An alternate method used was to set the two windows of the variable path cell so close together that fringes of interference resulted. This is because the refractive index of KRS5 ($n \simeq 2.38$) and of silicon ($n \simeq 3.4$) are high compared to those of liquids ($n \simeq 1.5$). Standing waves are created between the wave returning from the cell window far from the IR source and the incoming wave in the liquid (from the window close to the IR source). A damped wave is

observed by changing the distance between the windows until no power returns from the receding window. However, the precision of the "peak" positions determined by this method is inferior to the precision obtained above with a fixed path cell, scanning the frequency around the desired value (300 cm^{-1}, and 400 cm^{-1} respectively).

The UHF and microwave instrumentation for work up to 90 GHz has been described elsewhere.[13] For pure acetonitrile, at f = 50 GHz, a travelling wave technique has been used to determine the attenuation constant α (neper cm^{-1}),[13] whereas the power reflection method[13] has been used to determine $\lambda/2$ where λ is the wavelength in the liquid. Use of this hybrid method allows for increased precision at f = 50 GHz in the value of α for highly lossy liquids. In this case, the reflection technique allows detection of only two to three interference peaks before the wave returning from the metal reflector is completely absorbed.[13] From α and λ the values of ϵ' and ϵ'' are calculated using eq. (5) with the modification that for ϵ'

$$\epsilon' = \left(\frac{\lambda_o}{\lambda}\right)^2 \left[1 - \left(\frac{\alpha\lambda}{2\pi}\right)^2\right] + \left(\frac{\lambda_o}{\lambda_c}\right)^2 \qquad (6)$$

where $\lambda_c = 2b$ is the cut off wavelength of the rectangular waveguide of large dimension b. The refractive indices in the visible at the sodium line λ = 589.3 nm, for acetonitrile, benzonitrile and their mixtures with carbon tetrachloride at 25.0°C, have been measured with an Abbe precision refractometer with calibration charts (Bellingham and Stanley Ltd., London, U.K., distributed by Ercona Corp., Patchogue, NY). Table I reports the results of these measurements. Values of the static permittivity for acetonitrile, benzonitrile and their mixtures with carbon tetrachloride have been determined at 25°C and f = 1.1 MHz using a resonator technique and a cell of capacity $C_o = 0.56_6$ p Farad for the pure solvents and a cell of capacity C_o

= 5.20 p Farad for the CCl_4 mixtures rich in CCl_4.

Benzonitrile (Aldrich, Gold Label) was kept over molecular sieves (pre-dried in vacuo at 110°C) for a week and then distilled in vacuo in an all Pyrex column with no grease on the joints.

Acetonitrile (Aldrich, Gold Label) was purified in two ways. A portion was distilled over P_2O_5. Another portion was kept over molecular sieves for a week, and then distilled in the same column used for the benzonitrile except for the in vacuo conditions. The same results were obtained with the two distilled products. These results agreed with experimental results obtained in other laboratories, as shown below.

Carbon tetrachloride (Aldrich, Gold Label) was distilled in a column similar to those used for the nitriles after exposure over molecular sieves or P_2O_5.

The mixtures were prepared by weight on an analytical balance (10^{-4} g sensitivity) in volumetric flasks. Exposure to the atmosphere was limited during preparation of mixtures and filling the cells to 20-30 seconds overall.

Results and Discussion

a) Pure Liquids

Figure 3 reports the Cole-Cole plot of ϵ'' vs ϵ' for benzonitrile at 25°C. Previous literature data[2] at 21 ± 1°C and frequencies up to 36 GHz were interpreted by a single Debye relaxation function with $\epsilon_o = 25.6$, $f_r = 4.2$ GHz and $\epsilon_\infty = 3.85$. The present data extend to 88 GHz. The power reflected from a metal reflector vs distance from the mica window separating liquid and air is depicted in Figure 4A as attenuation (db) vs distance ℓ (inches). The position of the maxima and minima after ordinate correction for deviations

from the crystal linear square law gives the voltage reflection coefficient $\Gamma = \Gamma_\infty \exp(-0.11512\ (At - At_\infty))$ where At_∞ is the asymptotic value of the attenuation and

$$\Gamma_\infty^2 = \frac{(1 - \lambda/\lambda_o)^2 + (\alpha\lambda/2\pi)^2}{(1 + \lambda/\lambda_o)^2 + (\alpha\lambda/2\pi)^2} \tag{7}$$

Γ_∞ is obtained by successive approximations.[13] Figure 4B reports the quantities $-\ln[(\Gamma-\Gamma_\infty)/(1-\Gamma\Gamma_\infty)]$ *vs.* odd n's and $-\ln[(\Gamma_\infty\pm\Gamma)/(1\pm\Gamma\Gamma_\infty)]$ *vs.* even n's for the maxima and minima respectively, giving $(\alpha\lambda/2)$ from the slope of the solid line which was calculated by linear regression. The above details are reported to document the reliability of ϵ' and ϵ'' at f = 88 GHz.

The dashed line in Figure 3 is the tentative fit by a single Debye function with $\epsilon_o = 25.1$, $f_r = 4.5$ GHz and $\epsilon_\infty = 3.6$ in fair accord with the literature parameters[2] at 21 ± 1°C. From Figure 3, however, one may see that the fit of the Debye function with the data is not very satisfactory, especially at f = 8.31 and f = 13.80 GHz. An attempt has been made to use $n_{IR}^2 = 2.59$ at $\bar{\nu} = 300$ cm^{-1} (Table I) [in fair accord with the reported[14] value $n_{IR}^2 = 2.34$ at 70 cm^{-1} and 20°C], $\epsilon_o = 25.1$ fitting the data by a Cole-Davidson distribution function. This function gives ϵ' and ϵ'' according to the expressions:

$$\begin{aligned} \epsilon' &= (\epsilon_o - n_{IR}^2)\ \cos^\beta\phi\cos(\beta\phi) + n_{IR}^2 \\ \epsilon'' &= (\epsilon_o - n_{IR}^2)\ \cos^\beta\phi\sin(\beta\phi) \end{aligned} \tag{8}$$

with $\phi = \arctan(f/f_r)$, f_r the weighted average relaxation frequency and β the distribution parameter of the spectrum of relaxation times. Notice that the Cole-Davidson function, having fixed ϵ_o and n_{IR}^2, is a two parameters function in f_r and β, whereas the Debye function, having fixed ϵ_o, is a two parameter function in ϵ_∞ and f_r.

Figure 3 reports the Cole-Davidson function calculated with f_r = 3.1 GHz and β = 0.70. The fit appears satisfactory for frequencies above f = 8 GHz, but less satisfactory than the Debye function at f = 2.27 and f = 3.10 GHz. Using n_{IR}^2 = 2.59, measured at 300 cm^{-1}, means to include the process showing a maximum in the attenuation constant α observed at $\bar{\nu}$ = 55 cm^{-1} (f = 1650 GHz) in the family of relaxation processes to be described by the Cole-Davidson distribution function. Exclusion of the process observed at $\bar{\nu}$ = 55 cm^{-1} from the distribution implies the use of the value of n_{IR} at wavenumbers below $\bar{\nu}$ = 55 cm^{-1}, possibly the Debye value for ϵ_∞ = 3.60. Poley[2] noticed that the difference $\epsilon_\infty - n_{IR}^2$ was proportional to μ^2, the squared dipole moment of the molecule in the gas phase, for several C_6H_5-X benzene substituted liquids. Hill[5] derived an expression based on a librational resonant relaxation with molecules partially rotating over small energy barriers between shallow traps. Use of the Hill expression

$$\frac{\epsilon_\infty - n_{IR}^2}{\epsilon_0 - n_{IR}^2} = \frac{kT}{(1/2)I\omega^2} \tag{9}$$

gave $\bar{\nu} = \frac{\omega}{2\pi c}$ = 23 cm^{-1} which is about a factor of two from the value $\bar{\nu}$ = 55 cm^{-1} reported for benzonitrile by Gebbie et al.[3] In the above, I denotes the moment of inertia and c is the velocity of light in vacuo. The above is recalled to indicate that according to Hill's theory the value of ϵ_∞ = 3.85 at 21°C had to be retained from the Debye theory, and the value of n_{IR}^2 = 2.34, above the librational relaxation process, had to be used in order to calculate the frequency of the latter process, to be distinguished for rigid molecules from the fully rotational one of Debye nature. Other authors such as LeRoy[15] considered this distinction artificial and favored treating the whole ensemble of relaxation phenomena as various aspects of the same process. In this respect it should be noted that the sodium-D line refractive index of

benzonitrile at 20°C[16], is $n_D^{20} = 1.52892$ giving $(n_D^{20})^2 = 2.3376$, which is comparable to the Errera and Cartwright value[14] $n_{IR}^2 = 2.34$ at 70 cm^{-1}. Usage of the $n_{IR}^2 = 2.59$ at 25°C for the Cole-Davidson function includes the decay of both rotational and atomic polarization in the same distribution function.

This picture appears, however, to be oversimplified since our data show evidence of an additional process at $\bar{\nu} \simeq 378$ cm^{-1} for benzonitrile. Figure 5A reports the value of the digitized attenuation constant α (cm^{-1}) for a cell of thickness $\ell = 0.0212$ cm according to Eq. 4 for benzonitrile at wavenumbers encompassing the band centered at $\bar{\nu} \simeq 378$ cm^{-1}.

Notice that (see below, Table I) the refractive index of benzonitrile at $\bar{\nu} \simeq 300$ cm^{-1} is $n_{300} = 1.609$ at 25°C, a figure somewhat higher than the value obtained at $\bar{\nu} \simeq 400$ cm^{-1}, $n_{400} = 1.579$ at 25°C, and closer to the value of the refractive index in the visible at the D-doublet of sodium, $n_D = 1.525_8$ at 25°C. This would seem to imply that the above band, also common to acetonitrile, may be related to a distortion of the C-C≡N group common to both benzonitrile and acetonitrile. Figure 5B reports the attenuation coefficient α around $\bar{\nu} \simeq 378$ cm^{-1} for acetonitrile. From Table I below it is evident that the value of $n_{300} = 1.414$ at $\bar{\nu} \simeq 300$ cm^{-1} is higher than the value $n_{400} = 1.348$ at $\bar{\nu} \simeq 400$ cm^{-1}, which is close to $n_D = 1.3415$ at 25°C.

Now let us consider the results for acetonitrile for comparison with those for benzonitrile. Figure 6 reports the Cole-Cole plot of ϵ'' <u>vs</u> ϵ' for acetonitrile at 25°C. The data up to f = 80.5 GHz (from f = 0.38 GHz) can be described equally well by a single Debye relaxation function with parameters $\epsilon_0 = 35.8$, $\epsilon_\infty = 5.0$, and $f_r = 45$ GHz or by a Cole-Davidson distribution of relaxation functions with parameters $\epsilon_0 = 35.8$, $\epsilon_\infty = n_{IR}^2 = 2.00$, $f_r = 40$ GHz as the average relaxation frequency, and $\beta = 0.80$ the distribution parameter.

Figures 7A and 7B show the coefficient ϵ' and ϵ'' respectively vs the frequency f with the calculated values according to the two functions and associated parameters. Clearly, the choice between the two functions depends on the assumption of the ϵ_∞ value. Arnold et al.[10] have reported the existence of an absorption band peaked at ~97 cm^{-1}. We have noticed a band at 378 cm^{-1}. The value of $n_{IR}^2 = 1.82$ reported below for $\bar{\nu} \simeq 400$ cm^{-1} clearly encompasses the 97 cm^{-1} band as part of the family of processes described by the Cole-Davidson function. On the other hand $n_D^{25} = 1.3415$ for acetonitrile. Hence $(n_D^{25})^2 = 1.80$. This implies that the permittivity of acetonitrile at $\bar{\nu} \simeq 400$ cm^{-1} is only 1% higher than the visible value at 589.3 nm ($\bar{\nu} = 16{,}969$ cm^{-1}) where presumably the atomic polarization has already decayed. Hence, as in the case of benzonitrile described above, retention of the n_{IR}^2 as the value of ϵ_∞ implies incorporation of the relaxation of the atomic polarization and libration-resonant phenomena within the rotational phenomena described by the Cole-Davidson distribution. Notice that any objection based on the reliability of the data presented here for benzonitrile and acetonitrile is unfounded. We have close agreement with the data of Poley[2] in benzonitrile at 21 ± 1°C and agreement within experimental error with the data by Barthel[17] for acetonitrile, indicated on Figures 5 and 6 from 2.50 to 39.0 GHz. These data[17] are of excellent internal precision and were obtained by travelling wave interferometry in contrast with our data which were obtained by standing wave reflectometry with the exception of the data at f = 51.7 GHz. At present, there seems to be no clear preference for one over the other of the two alternatives presented above to describe the dielectric data. A detailed investigation of the gap between the far infrared region and the microwave region for both ϵ' and ϵ'' at many wavenumbers from 10 cm^{-1} (f = 300 GHz) to

300 cm^{-1} (f = 9000 GHz) appears necessary to clarify the nature of the processes involved in this region, case by case.

b) Mixtures with CCl_4

Figure 8A reports the squared refractive index at $\bar{\nu} \simeq 300$ cm^{-1} and $\bar{\nu} \simeq 400$ cm^{-1} vs the concentration of C_6H_5CN C(mol/dm^3) for the mixtures C_6H_5CN-CCl_4 investigated at t = 25°C. Table I reports the refractive indices at $\bar{\nu} \simeq 300$ cm^{-1} and at $\bar{\nu} \simeq 400$ cm^{-1} for benzonitrile-carbon tetrachloride mixtures at 25°C. The data can be represented by the linear regression:

$$n^2_{IR} = 2.38_2 + 2.34 \times 10^{-2} C_{C6H5CN};\ r^2 = 0.93 \text{ at } \bar{\nu} = 300 \text{ cm}^{-1}$$

$$n^2_{IR} = 2.37_9 + 1.31_1 \times 10^{-2} C_{C6H5CN};\ r^2 = 0.80 \text{ at } \bar{\nu} \simeq 400 \text{ cm}^{-1}$$

$$n^2_D = 2.12_7 + 2.15_1 \times 10^{-3} C_{C6H5CN};\ r^2 = 0.99 \text{ at } \bar{\nu} = 16{,}969 \text{ cm}^{-1}$$

with r^2 the determination coefficient.

Figure 9A displays the values of the attenuation coefficient α (cm^{-1}) vs the concentration of benzonitrile (expressed in mol/dm^3) at $\bar{\nu} \simeq 300$ cm^{-1} (f = 9,000 GHz) and at $\bar{\nu} \simeq 400$ cm^{-1} (f = 12,000 GHz) at 25°C. Table I reports the same data.

From the values of α and the interpolated values of n the values of the wavelength λ have been calculated. Then the values of ϵ' and ϵ'' at $\bar{\nu} \simeq 300$ cm^{-1} and $\bar{\nu} \simeq 400$ cm^{-1} have been calculated and reported in Table I. Table I reports the values of the refractive indices at the sodium line (λ = 589.3 nm, $\bar{\nu}$ = 16,969 cm^{-1}) for the benzonitrile-CCl_4 mixtures at 25°C. Figure 8A reports the refractive index n_D of the above mixtures vs C_{C6H5CN}.

Figure 8B reports the squared refractive index at $\bar{\nu} \simeq 300$ cm^{-1} and $\bar{\nu} \simeq 400$ cm^{-1} for the mixtures CH_3CN-CCl_4 investigated at 25°C vs the concentration of CH_3CN C(mol/dm^3). Table I reports the refractive index at $\bar{\nu} \simeq 300$ cm^{-1} and at $\bar{\nu} \simeq 400$ cm^{-1} for acetonitrile and acetonitrile-carbon tetrachloride

mixtures at 25°C. The data can be represented by the linear regressions:

$$n_{IR}^2 = 2.29_6 - 0.017\ C_{CH3CN} \text{ at } \bar{\nu} = 300\ cm^{-1};\ r^2 = 0.93$$

$$n_{IR}^2 = 2.28_5 - 0.023\ C_{CH3CN} \text{ at } \bar{\nu} = 400\ cm^{-1};\ r^2 = 0.97$$

$$n_D^2 = 2.12_4 - 1.741 \times 10^{-2}\ C_{CH3CN} \text{ at } \bar{\nu} = 16{,}969\ cm^{-1};\ r^2 = 0.998$$

with r^2 the determination coefficient. In the same Figure for CH_3CN the value of $n_D^2 = 1.80$ is reported, as well as the data for the CH_3CN-CCl_4 mixture. The data for n_{IR}^2 reported by Arnold et al.[10] at $\bar{\nu} \simeq 200\ cm^{-1}$ with their mole fractions converted to concentrations (mol/dm^3) by means of the mixture densities[18] are also reported. The data unfortunately appear to lack adequate precision. By taking the figure $n_{IR}^2 = 2.49$ at $\bar{\nu} \simeq 200\ cm^{-1}$ at face value for pure acetonitrile, it follows that starting from $\epsilon_\infty = 5$ (extrapolated from the microwave data ending at $\bar{\nu} = 2.7\ cm^{-1}$, $f = 81$ GHz), the value of n_{IR}^2 has dropped to 2.49 at $\bar{\nu} \simeq 200\ cm^{-1}$ and to 1.82 at $\bar{\nu} \simeq 400\ cm^{-1}$ quite close to the sodium line value of $n_D^2 = 1.80$. Hence at $\bar{\nu} \simeq 400\ cm^{-1}$ the atomic polarization of acetonitrile has already decayed. More data appear necessary from $\bar{\nu} = 10$-$300\ cm^{-1}$ to establish the profile of the decay of n_{IR}^2 with frequency. Figure 9B reports the values of the attenuation coefficient α vs the concentration of acetonitrile C_{CH3CN} (expressed in mol/dm^3) at $\bar{\nu} \simeq 300\ cm^{-1}$ ($f = 9000$ GHz) and $\bar{\nu} \simeq 400\ cm^{-1}$ ($f = 12{,}000$ GHz) (Table I) 25°C. From the values of α and n (Table I), the values of ϵ' and ϵ'' at $\bar{\nu} \simeq 300\ cm^{-1}$ and $\bar{\nu} \simeq 400\ cm^{-1}$ have been calculated for the mixtures investigated. The value of α at $\bar{\nu} \simeq 400\ cm^{-1}$ for pure acetonitrile is affected by the resonant band at $\bar{\nu} \simeq 378\ cm^{-1}$. It is therefore not reported.

Table I reports the value of the refractive indices at the sodium line ($\lambda = 589.3$ nm, $\bar{\nu} = 16{,}969\ cm^{-1}$) for the acetonitrile-$CCl_4$ mixtures at 25°C. These data of n_D are reported in Figure 8B vs C_{CH3CN}. Figure 10A reports the

representative plots of ϵ' and ϵ'' vs the frequency f of one of the C_6H_5CN-CCl_4 mixtures investigated by dielectric spectrometry at 25°C. A single Debye relaxation function is adequate to represent the data of the C_6H_5CN-CCl_4 mixtures.

Figure 10B presents representative plots of ϵ' and ϵ'' vs the frequency f and of ϵ'' vs ϵ' for one of the CH_3CN-CCl_4 mixtures investigated by dielectric spectrometry at 25°C. The concentrations of benzonitrile or of acetonitrile in the mixtures ranges from the diluted range to the more concentrated range up to $X_{C6H5CN} = 0.87$ and $X_{CH3CN} = 0.80$ respectively. It may be seen that as far as the dielectric data are concerned a single Debye relaxation function is capable of describing the data within experimental error. An attempt to fit the data by the Cole-Davidson distribution has also been made with fair results using the distribution parameter $\beta < 1$. Figures 10A and 10B report the Cole-Davidson functions and Table II the fitted parameters ϵ_o, f_r, and β where the n_{IR}^2 at $\bar{\nu} \simeq 300$ cm^{-1} has been used for ϵ_∞. Table II reports also all the parameters obtained by the Debye fit of the dielectric microwave data.

In order to check on the reliability of the extrapolated ϵ_o values from microwave data by the Debye function, measurements of the static permittivity at f = 1.1 MHz for benzonitrile, acetonitrile and their mixtures with CCl_4 at 25°C have been made by the dielectric resonator technique.

Figures 11A and 11B report the experimental data for ϵ_o together with the extrapolated values from microwave frequencies at the compositions investigated at 25°C. Table I reports the numerical values of the measured ϵ_o values for benzonitrile and acetonitrile mixtures respectively.

c) <u>C_6H_5CN and CH_3CN at Low Concentration in CCl_4. A Dielectric Study of the Dimerization of CH_3CN.</u>

The Böttcher equation[19] correlates the concentration C of a dipolar species of apparent dipole moment μ to the relaxation strength $\Delta\epsilon = \epsilon_o - \epsilon_\infty$ for that species

$$\epsilon_o - \epsilon_\infty = \frac{4\pi L \times 10^{-3}}{(1 - \alpha f)^2} \frac{\mu^2}{3kT} - \frac{3\epsilon_o}{2\epsilon_o + 1} C \qquad (10)$$

where L is Avogadro's number, α is the polarizability and f is the reaction field factor. The above expression can be rewritten, neglecting the polarizability α, and neglecting the reaction field factor f term [$(1-\alpha f)^2 \simeq 0.9$] with respect to unity, as

$$\phi(\epsilon) = (\epsilon_o - \epsilon_\infty) \frac{2\epsilon_o + 1}{3\epsilon_o} = \frac{4\pi L \times 10^{-3}}{3kT} \mu^2 c \qquad (11)$$

Figure 12A reports the Böttcher plot of $\phi(\epsilon)$ <u>vs</u> C for benzonitrile dissolved in CCl_4 up to C = 1.50 mol/dm^3. The solid straight line has been calculated by linear regression giving 50% statistical weight to zero intercept. The calculation gives $r^2 = 0.999$ and slope = 1.431 from which the apparent dipole moment $\mu = 4.8_3 \times 10^{-18}$ esu cm has been calculated. This figure is in fair accord with the value of $\mu = 4.1_4 \times 10^{-18}$ esu cm from the gas phase.[2]

Figure 12B reports the Böttcher plot of $\phi(\epsilon)$ <u>vs</u> C for acetonitrile dissolved in CCl_4 up to C = $\leq$ 0.5 mol/dm^3. A clear curvature of the plot suggests that some of the polar solute[20] exists in an apolar form. Application of the dimerization equilibrium[20]

$$\begin{gathered} 2CH_3CN \rightleftharpoons (CH_3CN)_2 \\ 2M \rightleftharpoons D \end{gathered} \qquad (12)$$

with the dimerization constant: $K_d = \frac{[D]}{[M]^2}$ and the conservation equation: $C_o = [M] + 2[D]$ with C_o the total concentration of CH_3CN, leads to the

relation $[M] = (-1 + \sqrt{1+8K_dC_o})/4K_d$. Figure 12B presents the function $\phi(\epsilon)$ vs [M], using the minimum value of K_d that linearizes the plot, namely $K_d = 0.35$. This figure is valid only as an order of magnitude given the relative insensitivity of the linearization of the plot. It is significant, however, that $K_d = 0.35$ is within the range of the standard error of the value $K_d = 0.56 \pm 0.27$ obtained by Popov[11] by NMR techniques for the dimerization of CH_3CN in CCl_4.

Equation 11 has been used successfully in a comparable concentration range for rather strongly interactive systems such as dipolar ion pairs in solution.[20,13] The correspondence with K_d obtained by NMR techniques[11] lends credence to the interpretation of the curvature of Figure 12B as arising from dimerization of acetonitrile. The present approach based on the NMR evidence of the dimerization of acetonitrile is an alternative to the use of the Kirkwood aggregation parameter[1] g expressing phenomenologically a similar concept.

Acknowledgements

The authors wish to acknowledge support from the Army Research Office, Durham, NC through grant #DAAL03-89-K-0148.

References

(1) Hill, N. *Dielectric Behavior and Molecular Structure*; Van Nostrand: London, 1969; Smyth, C. P. *Dielectric Behavior and Structure*; McGraw Hill: New York, NY, 1958.

(2) Poley, J. P. *Appl. Sci.* Res. B. **1955**, *4*, 337.

(3) Davies, M.; Pardoe G. W. F.; Chamberlain, J. E.; Gebbie, H. A. *Trans Faradat Soc.* **1968**, *64*, 847. Gebbie, H. A.; Stone, B. N. W.; Findlay, F. D.; Pyatt, E. C. *Nature* London **1965**, *205*, 377. Chamberlain, J. E.; Werner, E. B. C.; Gebbie, H. A.; Slough, W. *Trans. Far. Soc.* **1967**, *63*, 2605.

(4) Chantry, C. W.; Gebbie, H. A. *Nature*, London **1965**, *208*, 378.

(5) Hill, N. E. *Proc. Phys. Soc.* **1963**, *82*, 723.

(6) Lorentz, H. A. *The Theory of Electrons*; Dover Publ.: New York, 1915.

(7) Van Vleck, J. H.; Weisskopf, V. F. *Rev. Mod. Phys.* **1945**, *17*, 227.

(8) Cole, R. H. *Annual Rev. of Phys. Chem.* **1989**, *40*, 1.

(9) Wolynes, P. G. *J. Chem. Phys.* **1987**, *86*, 5133.

(10) Arnold, K. E.; Yarwood, J.; Price, A. H. *Molecular Physics* **1983**, *48*, 451.

(11) Boss, P. A. Mosier; Popov, A. I. *J. Am. Chem. Soc.* **1985**, *107*, 6168.

(12) U.S. Army Workshop on Capacitors for Pulse Power Application; Ashbury Park, NJ, Nov. 17-19, 1987.

(13) Farber, H.; Petrucci, S. *The Chemical Physics of Solvation*, Chapter 8, Vol. B, R. R. Dogonadze et al. Eds.; Elsevier: Amsterdam, 1986.

(14) Cartwright, C. H.; Errera, J. *Proc. Roy. Soc.* **1936**, *A154*, 138.

(15) LeRoy, Y. Doctorate of Sciences Thesis, University of Lille, France, 1967.

(16) *Handbook of Physics and Chemistry*; The Chemical Rubber Company: Cleveland, OH.

(17) Barthel, J. *J. Sol. Chem.*, in press.

(18) Accascina, F.; Petrucci, S.; Fuoss, R. M. *J. Am. Chem. Soc.* **1959**, *81*, 1301.

(19) Böttcher, C. J. F. *Theory of Dielectric Polarization*; Eselvier: Amsterdam, 1973.

(20) Delsignore, M.; Farber, H.; Petrucci, S. *J. Phys. Chem.* **1985**, *89*, 4968.

Table I

Infrared refractive index at $\bar{\nu} \simeq 300$ cm^{-1} and $\bar{\nu} \simeq 400$ cm^{-1}, attenuation coefficient α at $\bar{\nu} \simeq 300$ cm^{-1} and $\bar{\nu} = 400$ cm^{-1} and dielectric coefficients ϵ' and ϵ'' for CH_6CN-CCl_4 mixtures at 25°C. Visible refractive indices at $\lambda = 589.3$ nm; static permittivity ϵ_o.

X_{C6H5CN}	C_{C6H5CN} mol/dm^3	n_{300}	n^2_{300}	α (cm^{-1})	λ (cm)	ϵ'	ϵ'' *
$\bar{\nu} = 300$ cm^{-1}				$\lambda_o = 0.00333$ cm			
0.00	0.00	1.533	2.35	4.14	0.00217	2.35	0.00669
0.104	1.07	1.562	2.44	--	--	--	--
0.108	1.10	--	--	4.07	0.00215	2.40	0.00669
0.201	2.05	1.557	2.42	--	--	--	--
0.298	3.01	--	--	4.35	0.00213	2.45	0.00722
0.301	3.03	1.564	2.45	--	--	--	--
0.404	4.03	1.580	2.50	--	--	--	--
0.503	5.01	1.574	2.48	--	--	--	--
0.509	5.03	--	--	4.34	0.00211	2.50	0.00729
0.685	6.81	--	--	3.71	0.00209	2.54	0.00627
0.707	6.94	1.601	2.56	--	--	--	--
0.874	8.50	1.609	2.59	--	--	--	--
0.875	8.50	--	--	4.57	0.00208	2.57	0.00778
1.00	9.79_4	1.609	2.59	4.18	0.00207	2.59	0.00713

* The values of λ and α when not available from experimental n (and α), have been interpolated from the following functions:

$n_{300} = 1.543 + 7.40 \times 10^{-3}\ C_{C6H5CN}$; $r^2 = 0.92$

$n^2_{300} = 2.382 + 2.34 \times 10^{-2}\ C_{C6H5CN}$; $r^2 = 0.93$

$\alpha_{300} = 4.15 + 9.99 \times 10^{-3}\ C_{C6H5CN}$

Table I (continued)

X_{C6H5CN}	C_{C6H5CN} mol/dm^3	n_{400}	n^2_{400}	α (cm^{-1})	λ (cm)	ϵ'	ϵ'' *
$\bar{\nu}$ = 400 cm^{-1}				λ_o = 0.00250 cm			
0.00	0.00	1.525	2.33	0.328	0.00107	2.33	0.00026
0.108	1.10	--	--	0.703	0.00105	2.39	0.00056
0.144	1.46	1.557	2.42	--	--	--	--
0.298	3.01	--	--	2.22	0.00103	2.42	0.00176
0.301	3.03	1.562	2.44	--	--	--	--
0.404	4.03	1.561	2.44	--	--	--	--
0.503	5.01	1.572	2.47	--	--	--	--
0.509	5.03	--	--	4.13	0.00103	2.44	0.00330
0.685	6.81	--	--	4.73	0.00101	2.47	0.00376
0.707	6.94	1.572	2.47	--	--	--	--
0.874	8.50	1.574	2.48	--	--	--	--
0.875	8.50	--	--	7.00	0.00100	2.49	0.00555
1.00	9.794	1.579	2.49	6.78	0.00100	2.49	0.00537

* The values of λ and α when not available from experimental n (and α) have been interpolated from the following functions:

$n_{400} = 1.542 + 4.28 \times 10^{-3} C_{C6H5CN}$; $r^2 = 0.74$

$n^2_{400} = 2.37_9 + 1.31 \times 10^{-2} C_{C6H5CN}$; $r^2 = 0.80$

$\alpha_{400} = 1.64 \times 10^{-1} + 7.23 \times 10^{-1} C_{C6H5CN}$; $r^2 = 0.98$

Table I (continued)

X_{C6H5CN}	C_{C6H5CN} mol/dm^3	n_D	n^2_D	X_{C6H5CN}	C_{C6H5CN}	ϵ_O
0.00	0.000	1.4570_7	2.12	0.00	0.00	2.19
0.049	0.503	1.4610_9	2.13	0.0103	0.107	2.38
0.067	0.701	1.4630_8	2.14	0.0290	0.301	2.77
0.108	1.10	1.4668_4	2.15	0.0490	0.503	3.18
0.298	3.01	1.4825_1	2.20	0.0670	0.701	3.59
0.509	5.03	1.4988_0	2.25	0.108	1.00	4.22
0.685	6.81	1.5093_3	2.28	0.161	1.647	5.62
0.905	8.88	1.5213_0	2.31	0.300	3.06	8.83
1.00	9.79_4	1.5157_8	2.33	0.495	4.981	13.46
				0.707	7.027	18.54
				0.933	9.057	23.65
				1.00	9.794	25.33

$n^2_D = 2.12_7 + 2.151 \times 10^{-2}\ C_{C6H5CN}$; $r^2 = 0.99$

$\epsilon_O = 2.17 + 1.997\ C + 7.75_0 \times 10^{-2}\ C^2 - 3.87 \times 10^{-3}\ C^3$; $r^2 = 0.99$

Table I (continued)

Infrared refractive index at $\bar{\nu}$ = 300 cm^{-1} and $\bar{\nu}$ = 400 cm^{-1}, attenuation coefficient α at $\bar{\nu}$ = 300 cm^{-1} and dielectric coefficients ϵ' and ϵ'' for CH_3CN-CCl_4 mixtures at 25°C. Visible refractive indices at λ = 589.3 nm; static permittivity ϵ_o.

$\bar{\nu} \simeq 300\ cm^{-1}$ $\lambda_o = 0.00333$ cm

X_{CH3CN}	C_{CH3CN} mol/dm^3	n_{300}	n^2_{300}	α (cm^{-1})	λ (cm)	ϵ'	ϵ''
0.00	0.00	1.533	2.35	4.14	0.00142	2.35	0.00439
0.203	2.30	1.501	2.25	5.14	0.00222	2.25	0.00817
0.397	5.04	1.474	2.17	6.39	0.00226	2.17	0.00998
0.600	8.56	1.455	2.12	7.11	0.00229	2.12	0.0110
0.793	12.96	1.441	2.08	8.53	0.00231	2.08	0.0131
0.892	15.68	1.428	2.04	9.57	0.00233	2.04	0.0145
1.00	18.92	1.414	2.00	10.23	0.00236	2.00	0.0154

$$n^2_{IR}\ (300\ cm^{-1}) = 2.29_6 - 0.017\ C_{CH3CN},\ r^2 = 0.93$$

$\bar{\nu} \simeq 400\ cm^{-1}$ $\lambda_o = 0.00250$ cm

X_{CH3CN}	C_{CH3CN} mol/dm^3	n_{400}	n^2_{400}	α (cm^{-1})	λ (cm)	ϵ'	ϵ''
0.00	0.00	1.525	2.33	0.328	0.00107	2.33	0.00026
0.0478	0.503	1.496	2.24	--	0.00167	--	--
0.199	2.27	1.495	2.24	1.945	0.00167	2.24	0.00232
0.399	5.04	1.464	2.14	3.960	0.00171	2.14	0.00461
0.600	8.55	1.436	2.06	5.67	0.00174	2.06	0.00648
0.797	12.96	1.416	2.01	8.51	0.00177	2.01	0.00963
0.900	15.69	1.397	1.95	9.80	0.00179	1.95	0.0109
1.00	18.92	1.348	1.82	--	--	--	--

$$n^2_{IR}\ (400\ cm^{-1}) = 2.28_5 - 0.023\ C_{CH3CN},\ r^2 = 0.97$$

Table I (continued)

X_{CH3CN}	C_{CH3CN} mol/dm^3	n_D	$n^2{}_D$	X_{CH3CN}	C_{CH3CN}	ϵ_O
0.00	0.00	1.4570_7	2.12	0.00	0.00	2.19
0.200	2.29	1.4446_7	2.09	0.0134	0.139	2.52
0.396	5.04	1.4270_2	2.04	0.036	0.376_8	2.70
0.598	8.55	1.4043_0	1.97	0.0501	0.527_7	2.87
0.799	12.96	1.3758_7	1.89	0.254	2.95_9	6.18
0.898	15.69	1.3596_7	1.85	0.411	5.21_7	9.75
1.00	18.92	1.3414_8	1.80	0.597	8.46_3	15.63
				0.755	11.84	22.14
				0.844	14.09	26.59
				0.934	16.75	31.51
				1.00	18.92	35.55

$n^2{}_D = 2.12_4 - 1.741 \times 10^{-2}\ C_{CH3CN}$; $r^2 = 0.998$

$\epsilon_O = 2.26 + 1.143\ C + 6.668 \times 10^{-2}\ C^2 - 1.811 \times 10^{-3}\ C^3$; $r^2 = 0.99$

Table II

Collected dielectric parameters ϵ_o, ϵ_∞ and f_r according to the Debye relaxation function and ϵ_o, $\epsilon_\infty = n_{IR}^2$ (300), f_r and β according to the Cole-Davidson distribution function when used for C_6H_5CN-CCl_4 mixtures at 25°C.

X_{C6H5CN}	C_{C6H5CN}	ϵ_o	ϵ_∞	f_r (GHz)
Debye Function				
0.0489	0.50	3.28	2.26	6.2
0.0730	0.75	3.77	2.32	6.2
0.0978	1.00	4.35	2.35	6.2
0.145	1.50	5.50	2.60	5.3
0.297	3.00	8.70	2.70	4.5
0.499	5.00	13.6	2.85	5.0
0.866	8.50	22.6	3.00	5.0
1.00	9.79	25.1	3.60	4.5

X_{C6H5CN}	C_{C6H5CN}	ϵ_o	$\epsilon_\infty = n_{IR}^2$	f_r (GHz)	β
Cole-Davidson Function					
0.0489	0.50‡				
0.0730	0.75‡				
0.0978	1.00‡				
0.145	1.50	5.50	2.42	4.5	0.90
0.297	3.00	8.70	2.45	4.5	0.90
0.499	5.00	13.6	2.48	4.5	0.85
0.866	8.50	22.6	2.59	4.2	0.90
1.00	9.79	25.1	2.59	3.1	0.70

‡ For the mixtures of composition $X_{C6H5CN} \leq 0.1$ the Debye relaxation function describes the data adequately.

Table II (continued)

Collected dielectric parameters ϵ_0, ϵ_∞ and f_r according to the Debye relaxation function† and ϵ_0, $\epsilon_\infty = n_{IR}^2$ (300), f_r and β according to the Cole-Davidson distribution function when used for CH_3CN-CCl_4 mixtures at 25°C.

X_{CH3CN}	C_{CH3CN}	ϵ_0	ϵ_∞	f_r (GHz)
Debye Function				
0.00966	0.100	2.37	2.24	30
0.0193	0.200	2.51	2.24	30
0.0290	0.303	2.64	2.28	30
0.0390	0.400	2.74	2.30	30
0.0478	0.503	2.85	2.30	30
0.199	2.29	5.20	2.80	20
0.398	5.04	9.60	3.70	23
0.598	8.55	15.8	4.80	28
0.796	12.98	24.5	5.00	30
1.00	18.92	35.8	5.00	45

X_{CH3CN}	C_{CH3CN}	ϵ_0	$\epsilon_\infty = n_{IR}^2$	f_r (GHz)	β
Cole-Davidson Function					
0.199	2.29	5.20	2.25	15	0.60
0.398	5.04	9.50	2.17	17	0.60
0.598	8.55	15.4	2.12	22	0.65
0.796	12.98	24.5	2.08	19	0.65
1.00	18.92	35.8	2.00	40	0.80

† Concentrations are reported with three digits in order to avoid round-off errors in recalculations by others. The values of ϵ_0 and ϵ_∞ are affected by an average error of ± 1%. (The value of ϵ_∞ for pure acetonitrile by ± 10%. The values of f_r by an average error of ± 5%. The value of β by ± 5%.)

Appendix

Fringes in the interference pattern between two parallel plates of transparent material are caused by interference between radiation which is transmitted through the cell and radiation which is reflected from the inner surface of the cell, away from the source. The path difference between the two rays equals 2ℓ, with ℓ the apparent distance between the two plates, for normal incidence where

$$2\ell = \frac{N}{\bar{\nu}_2 - \bar{\nu}_1} = \frac{1}{\frac{d\bar{\nu}}{dN}}$$

with N the number of fringes between $\bar{\nu}_1$ and $\bar{\nu}_2$. The quantity $d\bar{\nu}/dN$ is inversely proportional to the refractive index of the medium between the two parallel plates. Thus by measuring the number of fringes with the cell filled first with a liquid of average refractive index n (between $\bar{\nu}_1$ and $\bar{\nu}_2$), and then with air (n_o=1)

$$\ell = \frac{n}{\frac{2d\bar{\nu}}{dN}} \quad , \quad \ell_o = \frac{1}{\frac{2d\bar{\nu}}{dN}}$$

we obtain $(\ell/\ell o) = n$.* The requirement for the method to work is that the window refractive index must be much larger than that of the liquid under study. Thallium bromoiodide (KRS5) with $n \simeq 2.38$ in the range 5000-300 cm^{-1} and silicon with $n \simeq 3.4$ in the ranges 5000-2000, ~500-30 cm^{-1} are suitable window materials.

* For an account of the method see J. Fahrenfort in "Infrared Spectroscopy and Molecular Structure," Edited by M. Davies, Elsevier Publ. Co., Amsterdam, 1963, Chapter XI.

Appendix

The explanation of the appearance of a refractive index in the expression above is easily achieved using a monocromatic radiation, for simplicity.

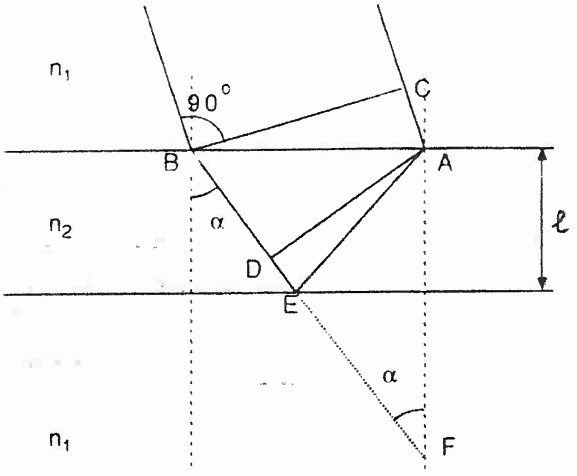

Take two parallel plates of refractive index n_1, with a medium of refractive index $n_2<n_1$ interposed in between. The difference in optical path between the refracted ray (at B) and reflected ray and the one incident at A is $\delta=n_2(BE+EA)-n_1CA$.

Also CA and BD are proportional to the velocities v_1 and v_2

$$\frac{CA}{BD}=\frac{v_1}{v_2}=\frac{v_1}{v_0}=\frac{v_0}{v_2}=\frac{n_2}{n_1}\ ,\ \text{with } v_0 = 3 \times 10^{10} \text{ cm s}^{-1}.$$

Therefore $n_1CA = n_2BD$
$\delta=n_2(BE+EA)-n_2BD$; but $BE-BD=DE$
$\delta=n_2(DE+EA)$; but $DE+EA=DF$
(as $EA=EF$) $DF=AF\cos\alpha=2\ell\cos\alpha$
$\delta=2\ell n_2\cos\alpha$ or
$\delta=2\ell n_2$ for normal incidence ($\alpha=0$)

One can now substitute air as the medium in between the plates with $n_0=1$ and α', having
$\delta'=(BE'+E'A')-n_1C'A'$
$\frac{C'A'}{BD'}=\frac{v_1}{v_0}=\frac{1}{n_1}$
$n_1C'A'=BD'$
$\delta'=BE'+E'A'-BD'$; but $BE'-BD'=D'E'$
$\delta'=D'E'+E'A'$; but $D'E'+E'A'=D'F'$
$D'F'=A'F'\cos\alpha'=2\ell\cos\alpha'$
$\delta'=2\ell\cos\alpha'$ or
$\delta'=2\ell$ for normal incidence ($\alpha'=0$)
Then $\delta/\delta'=n_2$,
where δ and δ' are the difference in path length for destructive interference, namely for an odd number of half wavelengths.

List of Figures

Fig 9A Attentuation coefficient α (cm^{-1}) vs concentration of benzonitrile C (mole/dm^3) at $\bar{\nu}$ = 300 cm^{-1} and $\bar{\nu}$ = 400 cm^{-1} for benzonitrile-CCl_4 mixtures at 25°C.

Fig. 9B Attentuation coefficient α (cm^{-1}) vs concentration of acetonitrile C (mole/dm^3) at $\bar{\nu}$ = 300 cm^{-1} and $\bar{\nu}$ = 400 cm^{-1} at 25°C for CH_3CN-CCl_4 mixtures.

Fig. 10A Plot of ϵ' and of ϵ'' vs f for the C_6H_5CN-CCl_4 mixtures of composition X_{C6H5CN} = 0.866 (C = 8.50 mol dm^{-3}) at 25°C. The dashed line is the Debye and the solid line is the Cole-Davidson function with the parameters reported in Table II.

Fig. 10B Plot of ϵ' and of ϵ'' vs f for the CH_3CN-CCl_4 mixture of composition X_{CH3CN} = 0.598 (C = 8.55 mol dm^{-3}) at 25°C. The dashed line is the Debye and the solid line is the Cole-Davidson function with the parameters reported in Table II.

Fig. 11A Experimental ϵ_0 values and ϵ_0 values extrapolated from microwave spectra for C_6H_5CN-CCl_4 at the compositions investigated at 25°C.

Fig. 11B Experimental ϵ_0 values and ϵ_0 values extrapolated from microwave spectra for CH_3CN-CCl_4 at the compositions investigated at 25°C.

Fig. 12A Böttcher plot of $\phi(\epsilon) = (\epsilon_0 - \epsilon_\infty) \frac{2\epsilon_0 + 1}{3\epsilon_0}$ vs the total concentration of benzonitrile for the C_6H_5CN-CCl_4 mixtures of concentration $C_{C6H5CN} \leq 1.5$ M at 25°C.

Fig. 12B Böttcher plot of $\phi(\epsilon) = (\epsilon_0 - \epsilon_\infty) \frac{2\epsilon_0 + 1}{3\epsilon_0}$ vs the total concentration of acetonitrile and vs (M) the concentration of undimerized acetonitrile (with a dimerization constant K_d = 0.35) for CH_3CN-CCl_4 mixtures at 25°C.

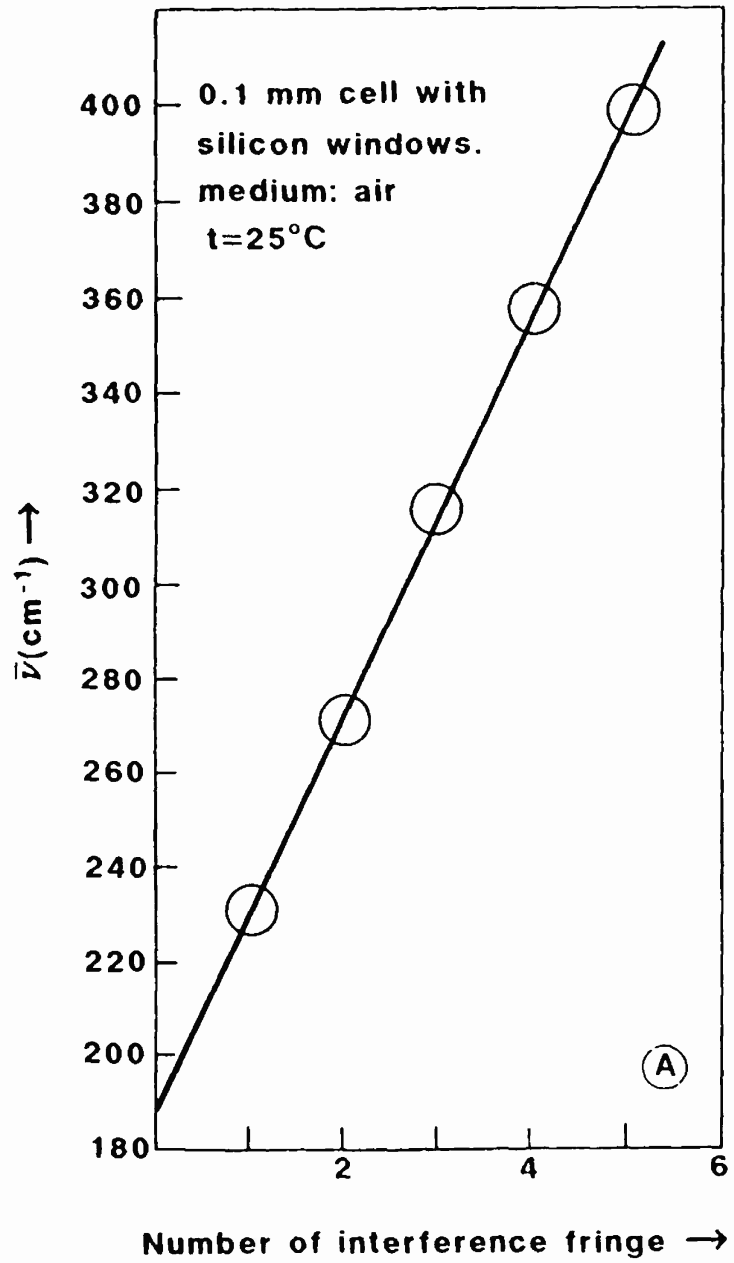
0.1 mm cell with
silicon windows.
medium: air
t=25°C
400
380
360
340
320
300
280
260
240
220
200
180
$\bar{\nu}$(cm^{-1}) →
2
4
6
A
Number of interference fringe →

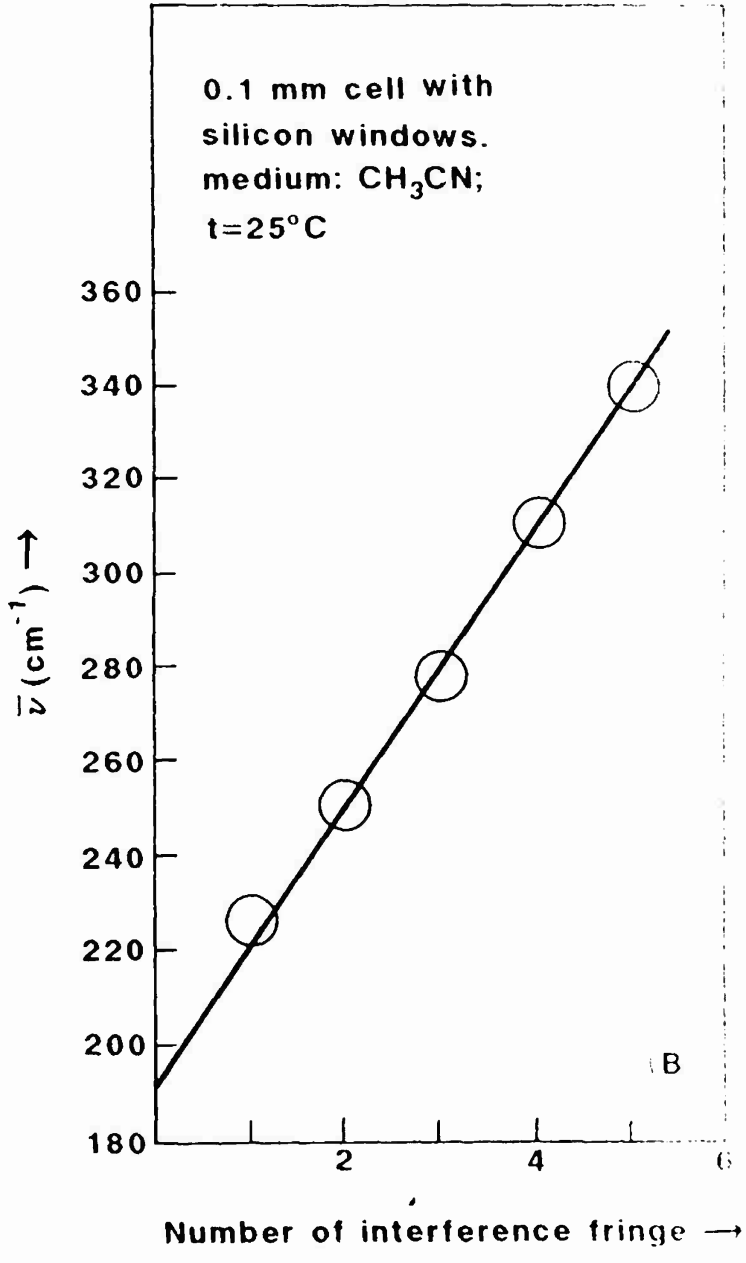
0.1 mm cell with
silicon windows.
medium: CH_3CN;
t=25°C
360
340
320
300
280
260
240
220
200
180
$\bar{\nu}$ (cm^{-1}) →
2
4
B
Number of interference fringe →

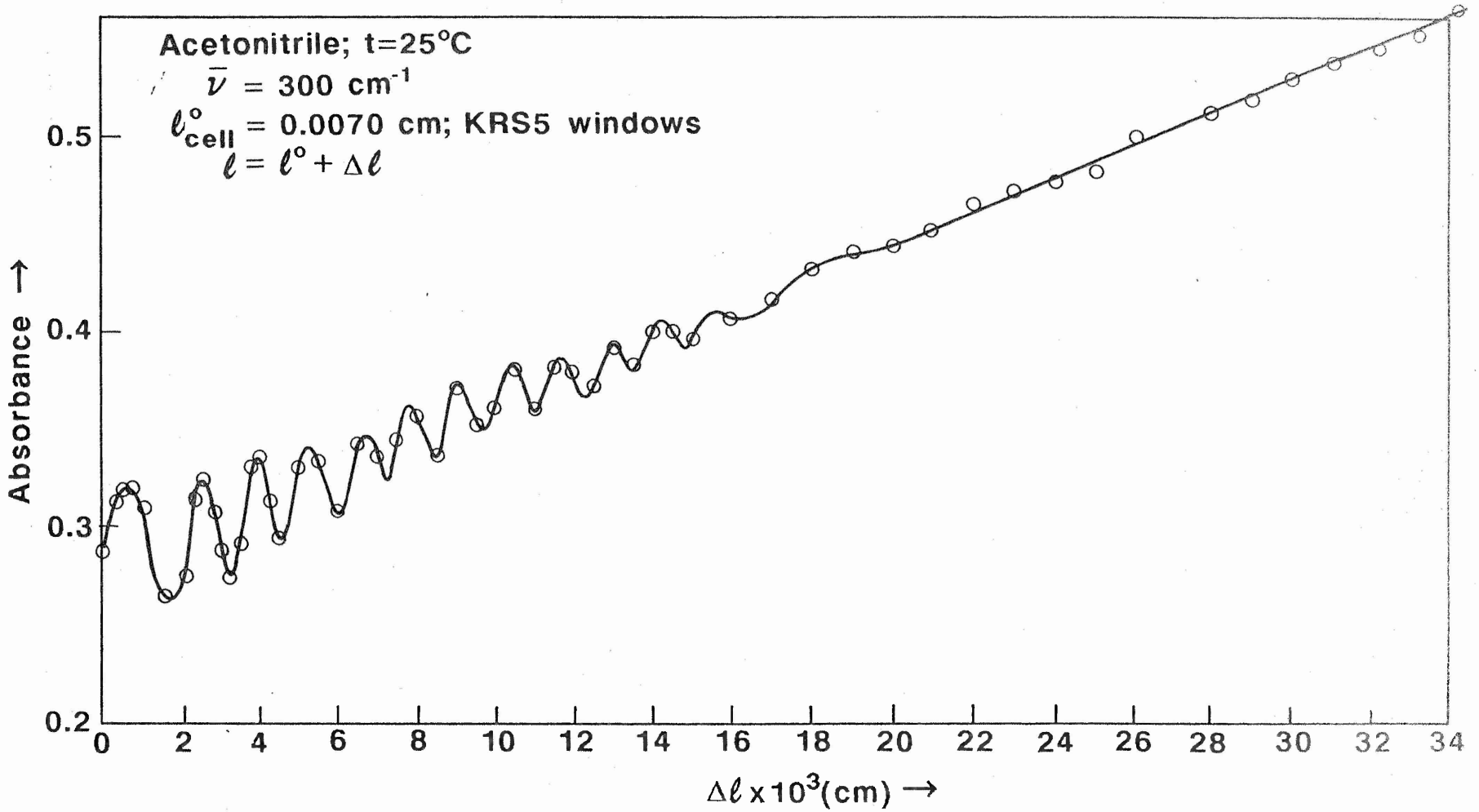
Acetonitrile; t=25°C
$\bar{\nu}$ = 300 cm^{-1}
ℓ°_{cell} = 0.0070 cm; KRS5 windows
$\ell = \ell^{\circ} + \Delta\ell$
Absorbance →
0.2
0.3
0.4
0.5
0
2
4
6
8
10
12
14
16
18
20
22
24
26
28
30
32
34
$\Delta\ell \times 10^3$(cm) →

F1%2

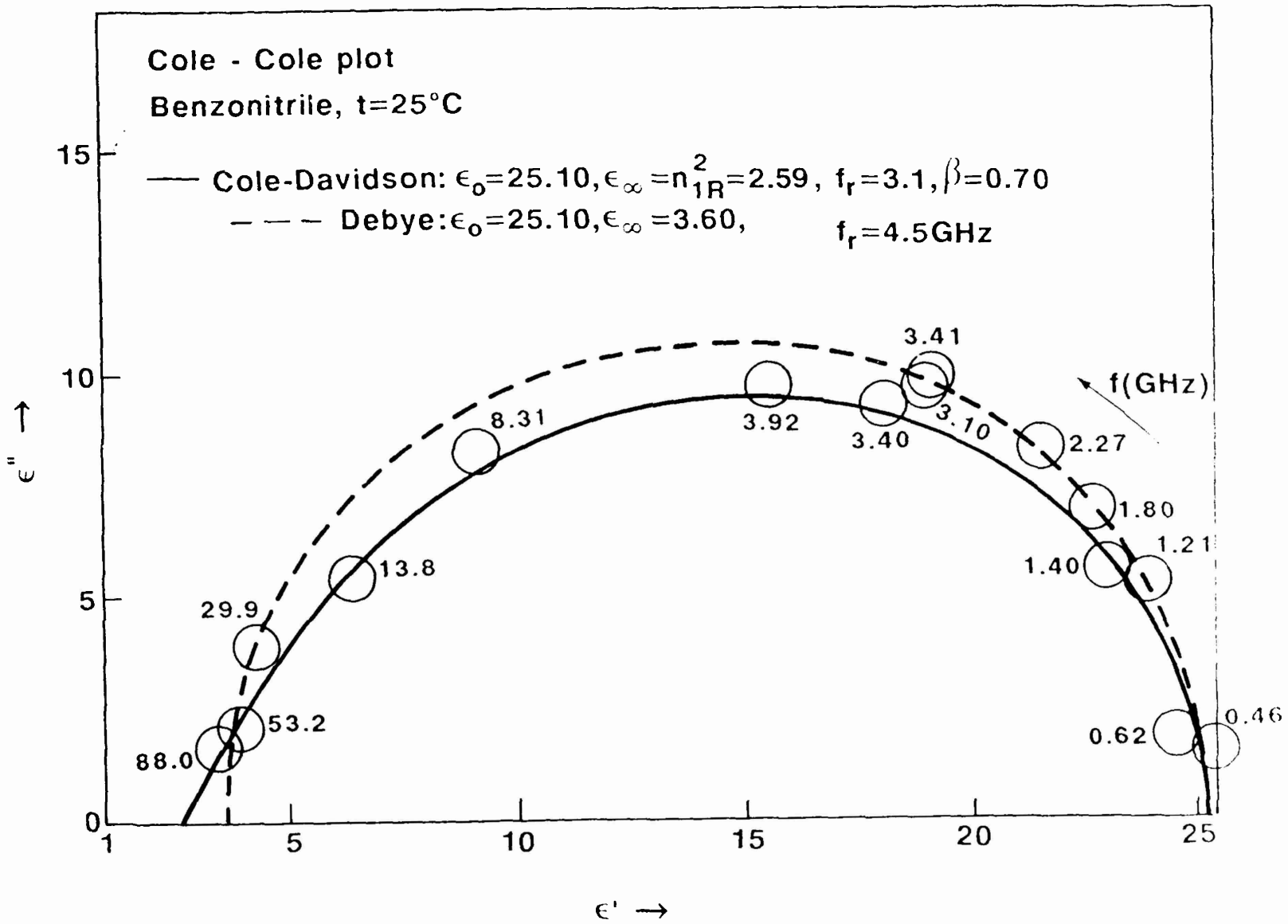
Cole - Cole plot
Benzonitrile, t=25°C
Cole-Davidson: ϵ_o=25.10, $\epsilon_\infty = n_{1R}^2$=2.59, f_r=3.1, β=0.70
Debye: ϵ_o=25.10, ϵ_∞=3.60, f_r=4.5GHz
f(GHz)
88.0
53.2
29.9
13.8
8.31
3.92
3.41
3.40
3.10
2.27
1.80
1.40
1.21
0.62
0.46
ϵ'' →
ϵ' →
0
5
10
15
1
5
10
15
20
25

Fig 2

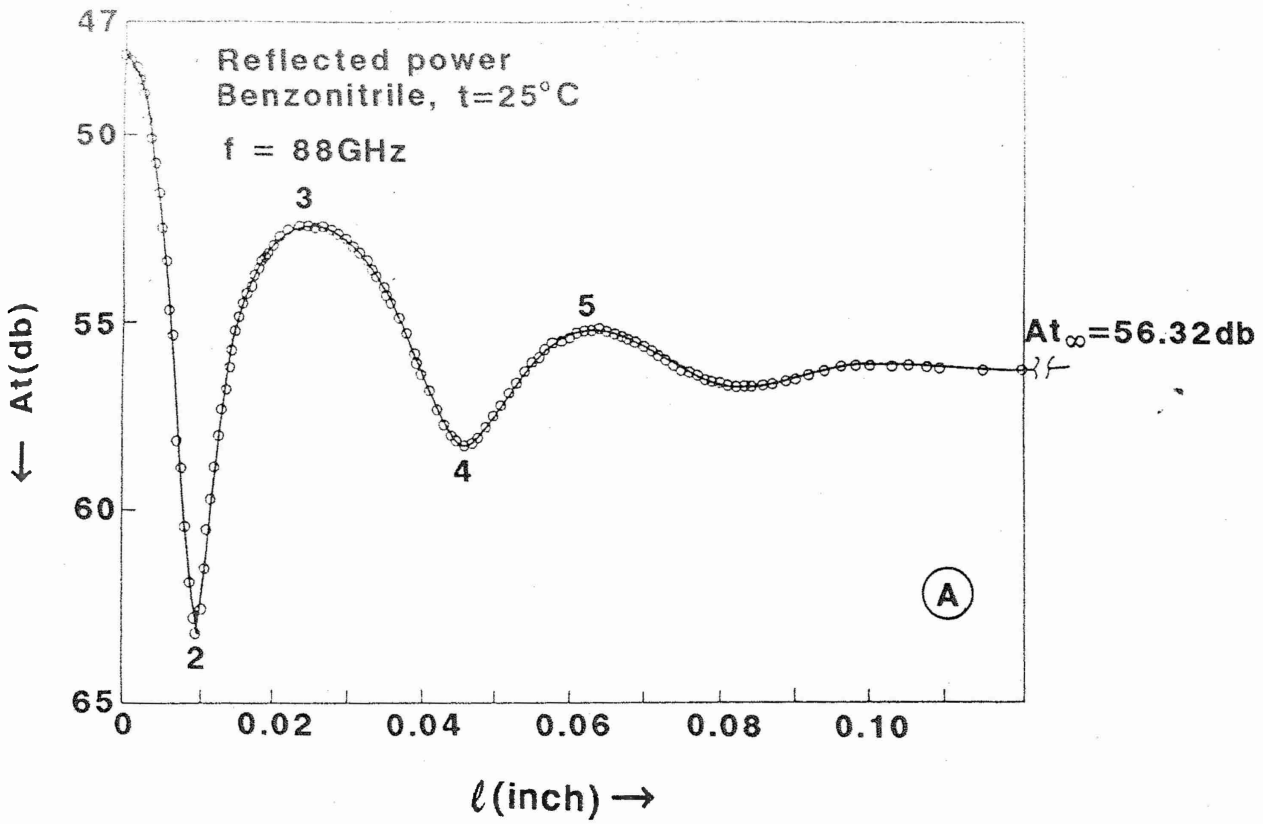
Reflected power
Benzonitrile, t=25°C
f = 88GHz
47
50
55
60
65
← At(db)
0
0.02
0.04
0.06
0.08
0.10
ℓ(inch) →
2
3
4
5
At∞=56.32db
A

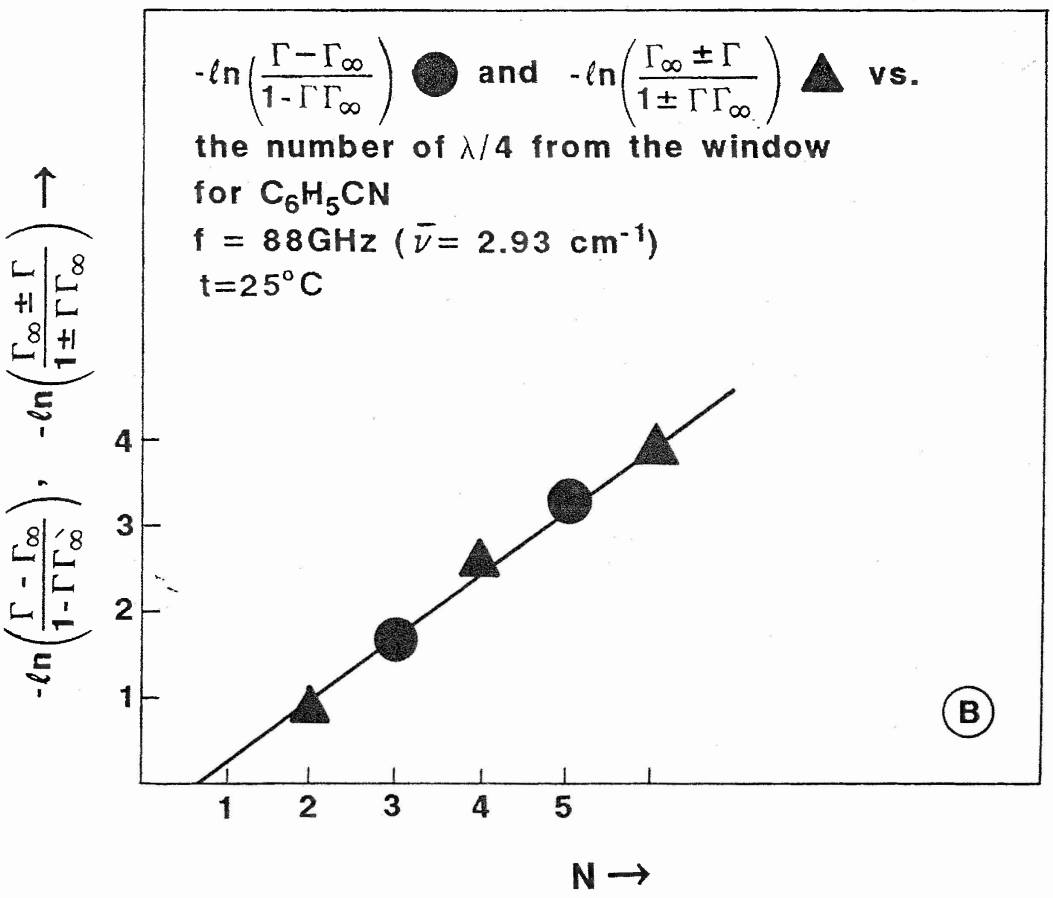
-ℓn((Γ−Γ∞)/(1−ΓΓ∞)) ● and -ℓn((Γ∞±Γ)/(1±ΓΓ∞)) ▲ vs.
the number of λ/4 from the window
for C6H5CN
f = 88GHz (ν̄= 2.93 cm-1)
t=25°C
-ℓn((Γ−Γ∞)/(1−ΓΓ∞)), -ℓn((Γ∞±Γ)/(1±ΓΓ∞)) →
1
2
3
4
5
N →
B

Fig. 4

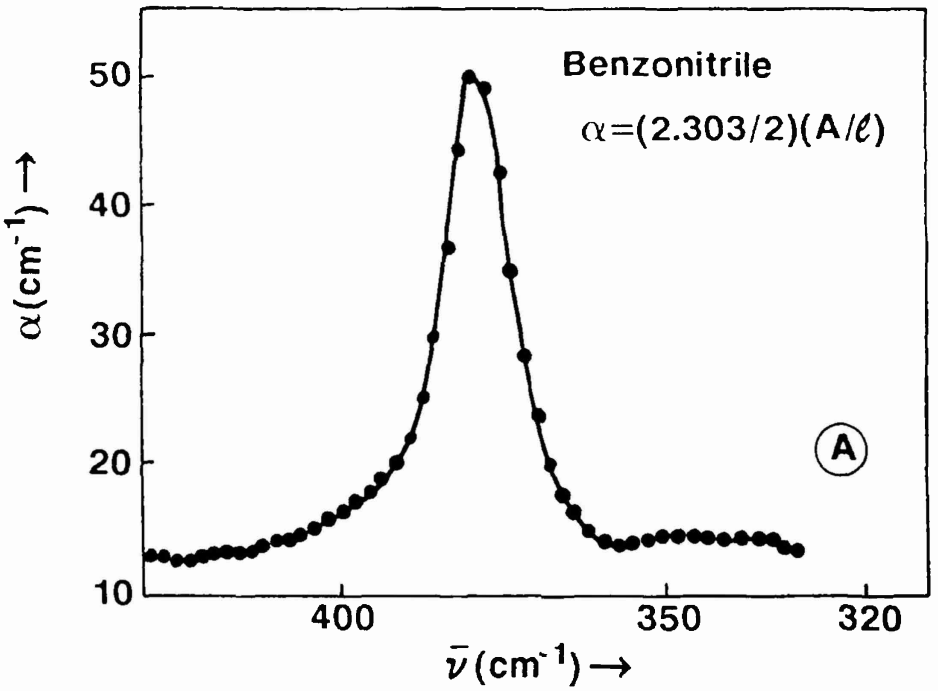
Benzonitrile
α=(2.303/2)(A/ℓ)
A
α(cm⁻¹) →
50
40
30
20
10
400
350
320
ν̄ (cm⁻¹) →

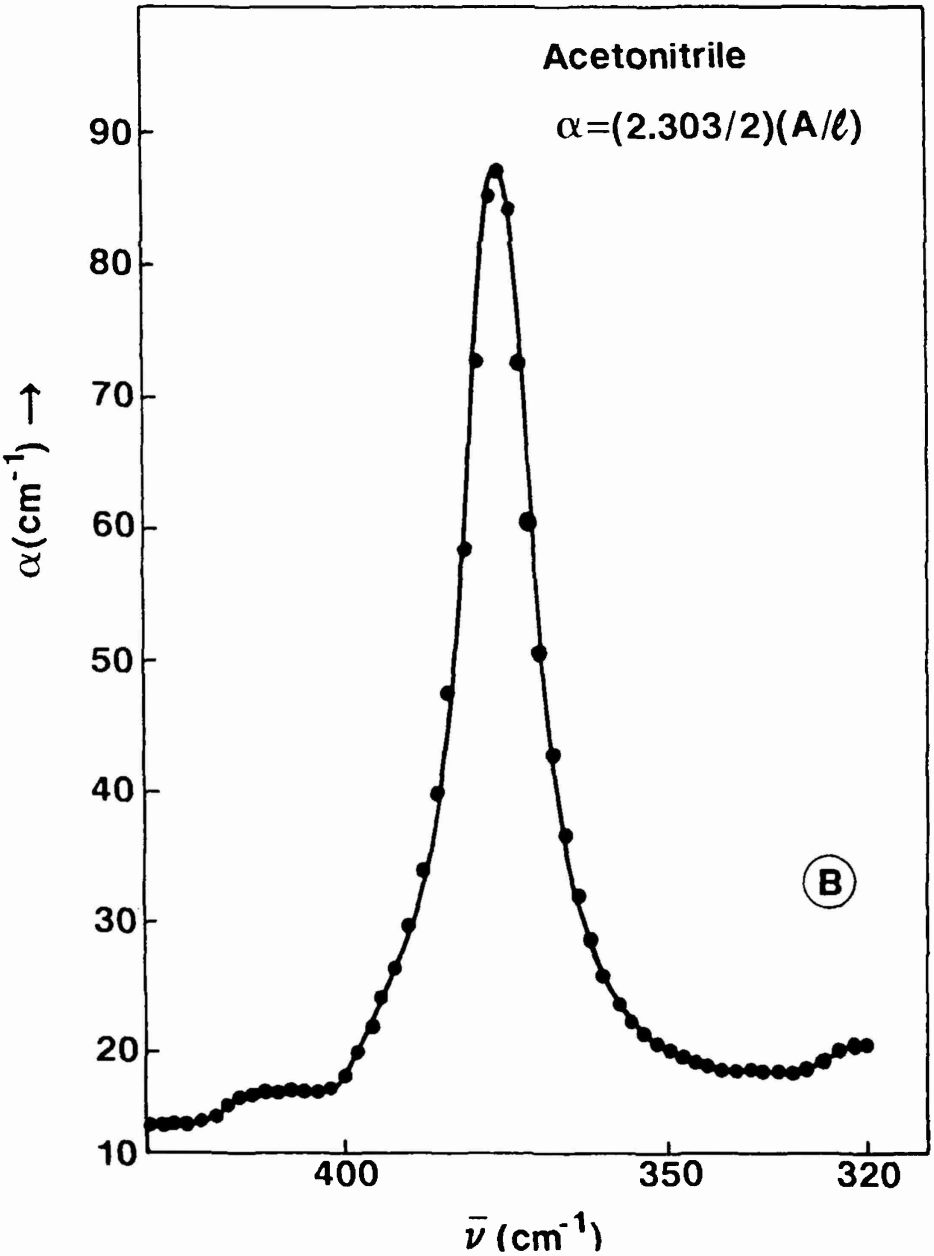
Acetonitrile
α=(2.303/2)(A/ℓ)
B
α(cm⁻¹) →
90
80
70
60
50
40
30
20
10
400
350
320
ν̄ (cm⁻¹)

Fig. 5

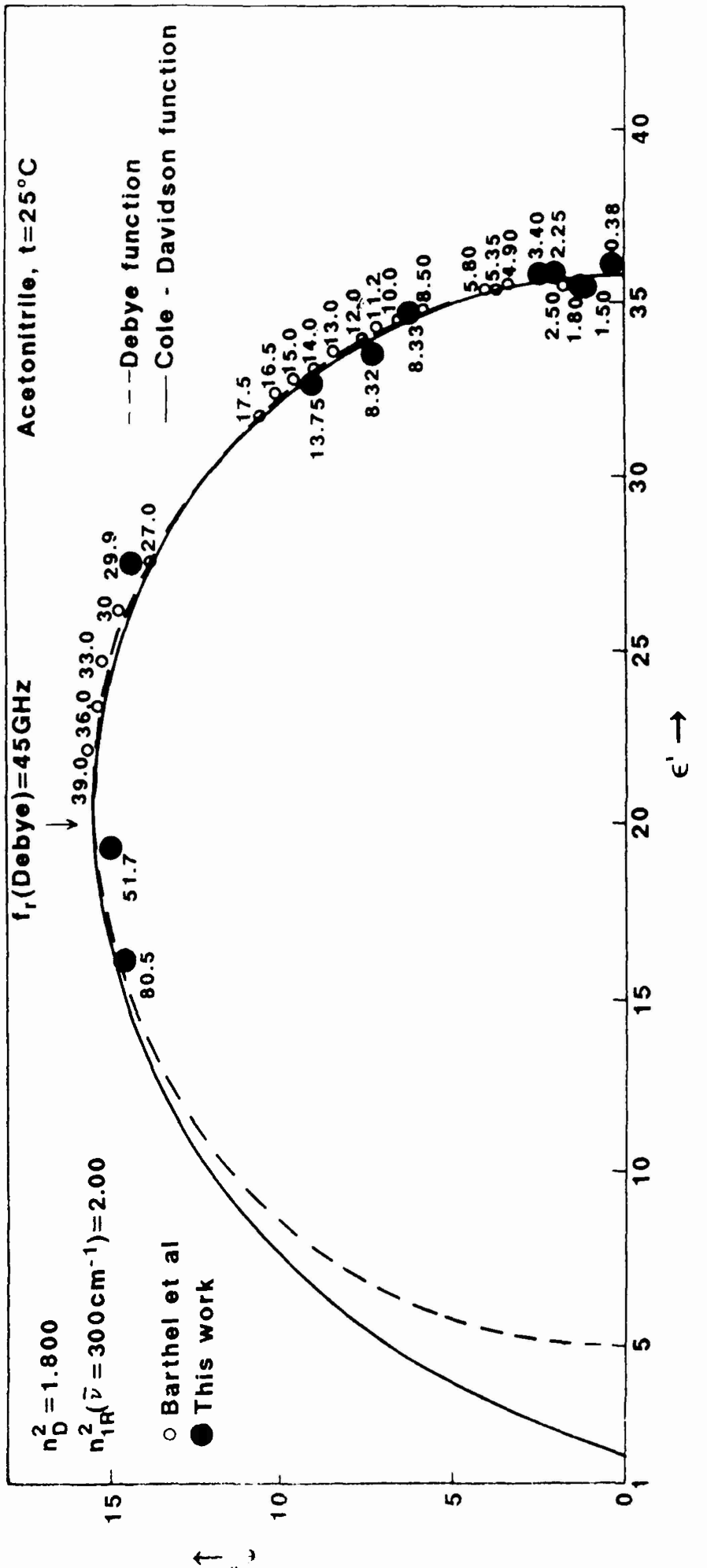
Acetonitrile, t=25°C
f_r(Debye)=45GHz
---Debye function
——Cole - Davidson function
n_D^2=1.800
$n_{IR}^2(\tilde{\nu}=300cm^{-1})$=2.00
○ Barthel et al
● This work
ε'' →
ε' →
0
5
10
15
20
25
30
35
40
80.5
51.7
39.0
36.0
33.0
30
29.9
27.0
17.5
16.5
15.0
14.0
13.75
13.0
12.0
11.2
10.0
8.50
8.33
8.32
5.80
5.35
4.90
3.40
2.25
2.50
1.80
1.50
0.38

Fig 6

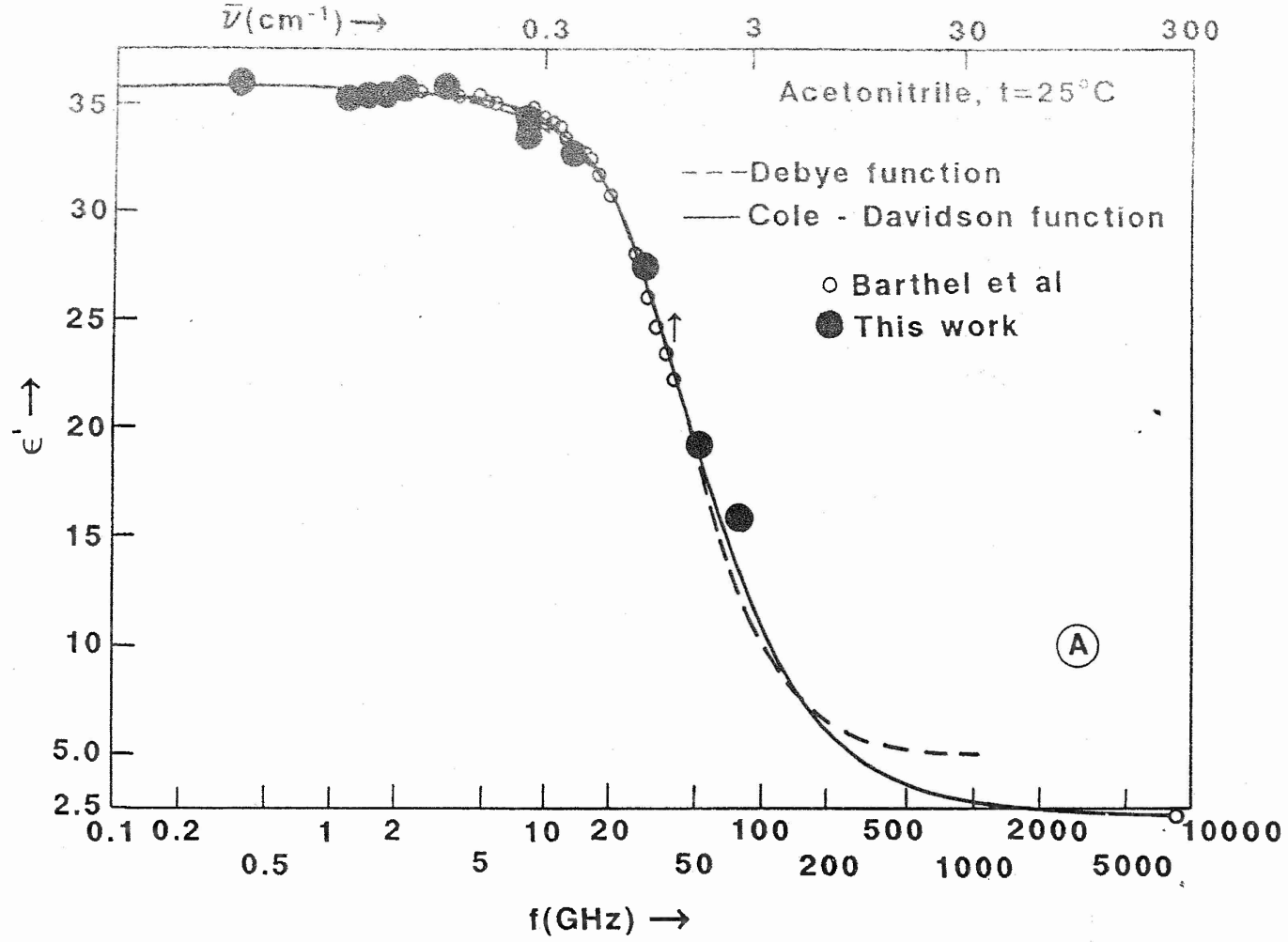
$\bar{\nu}$(cm^{-1}) →
0.3
3
30
300
Acetonitrile, t=25°C
---Debye function
——Cole - Davidson function
○ Barthel et al
● This work
ε' ↑
35
30
25
20
15
10
5.0
2.5
0.1 0.2 0.5 1 2 5 10 20 50 100 200 500 1000 2000 5000 10000
f(GHz) →
A

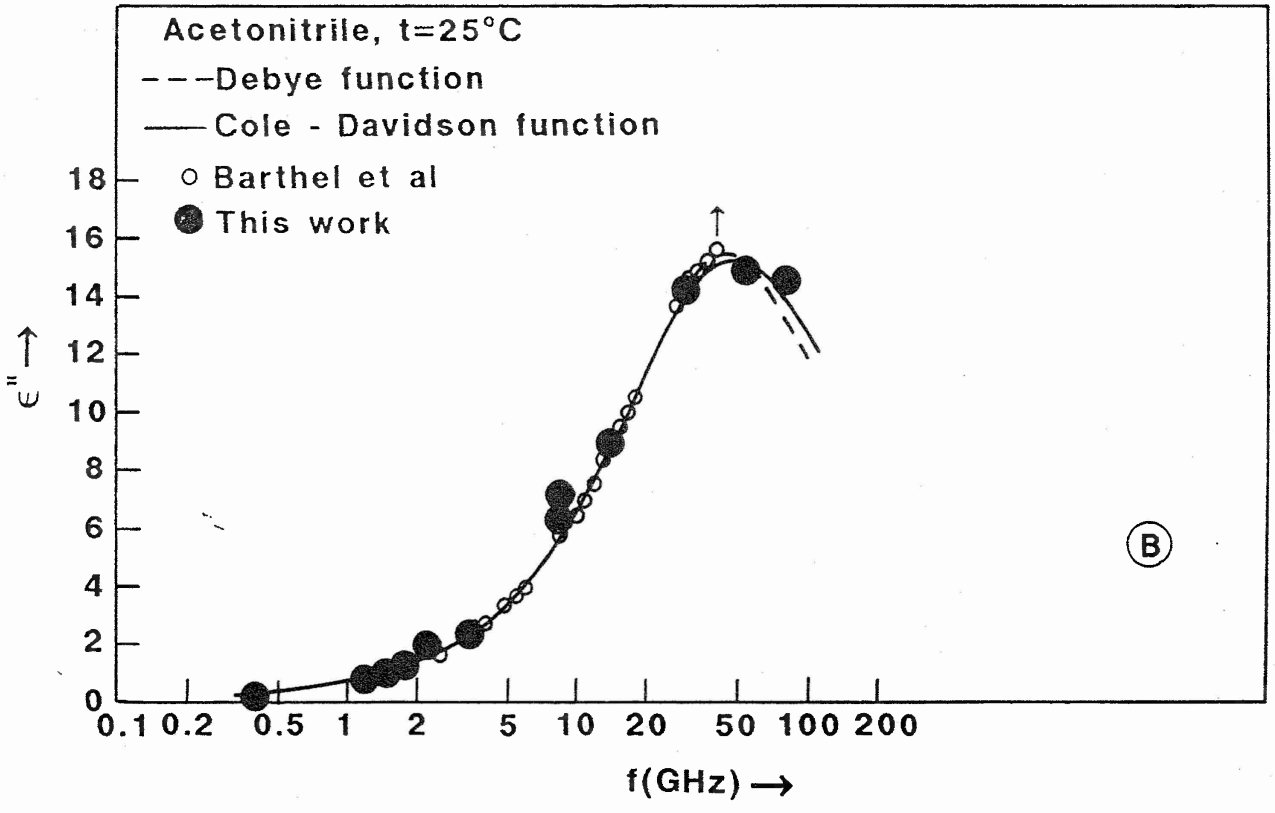
Acetonitrile, t=25°C
---Debye function
——Cole - Davidson function
○ Barthel et al
● This work
ε'' ↑
18
16
14
12
10
8
6
4
2
0
0.1 0.2 0.5 1 2 5 10 20 50 100 200
f(GHz) →
B

Fig 7

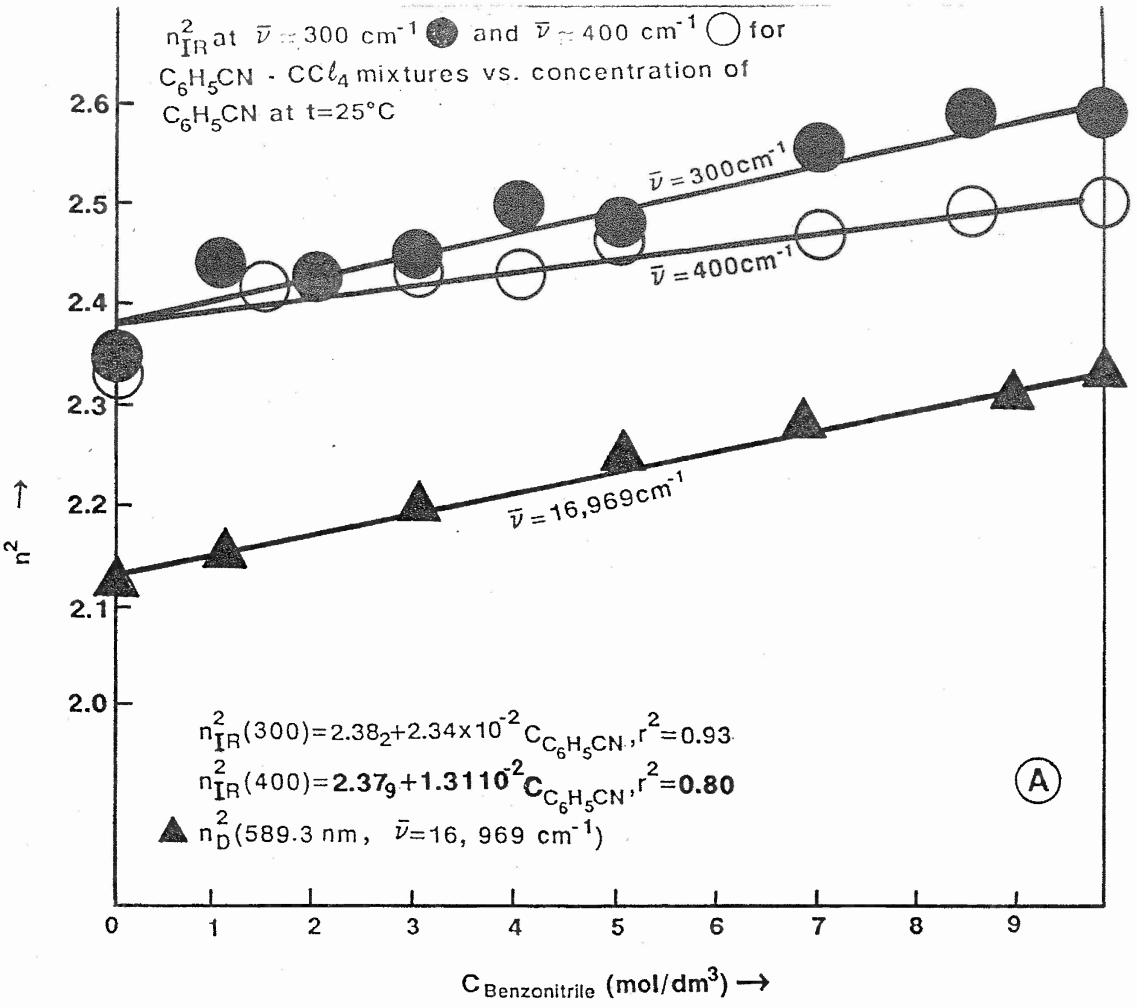
n^2_{IR} at $\bar{\nu} \simeq 300\ cm^{-1}$ ● and $\bar{\nu} \simeq 400\ cm^{-1}$ ○ for
C_6H_5CN - $CC\ell_4$ mixtures vs. concentration of
C_6H_5CN at t=25°C
$\bar{\nu} = 300 cm^{-1}$
$\bar{\nu} = 400 cm^{-1}$
$\bar{\nu} = 16{,}969 cm^{-1}$
$n^2_{IR}(300) = 2.38_2 + 2.34 \times 10^{-2} C_{C_6H_5CN}, r^2 = 0.93$
$n^2_{IR}(400) = 2.37_9 + 1.31 10^{-2} C_{C_6H_5CN}, r^2 = 0.80$
▲ n^2_D(589.3 nm, $\bar{\nu}$=16, 969 cm^{-1})
A
n^2 →
$C_{Benzonitrile}$ (mol/dm³) →

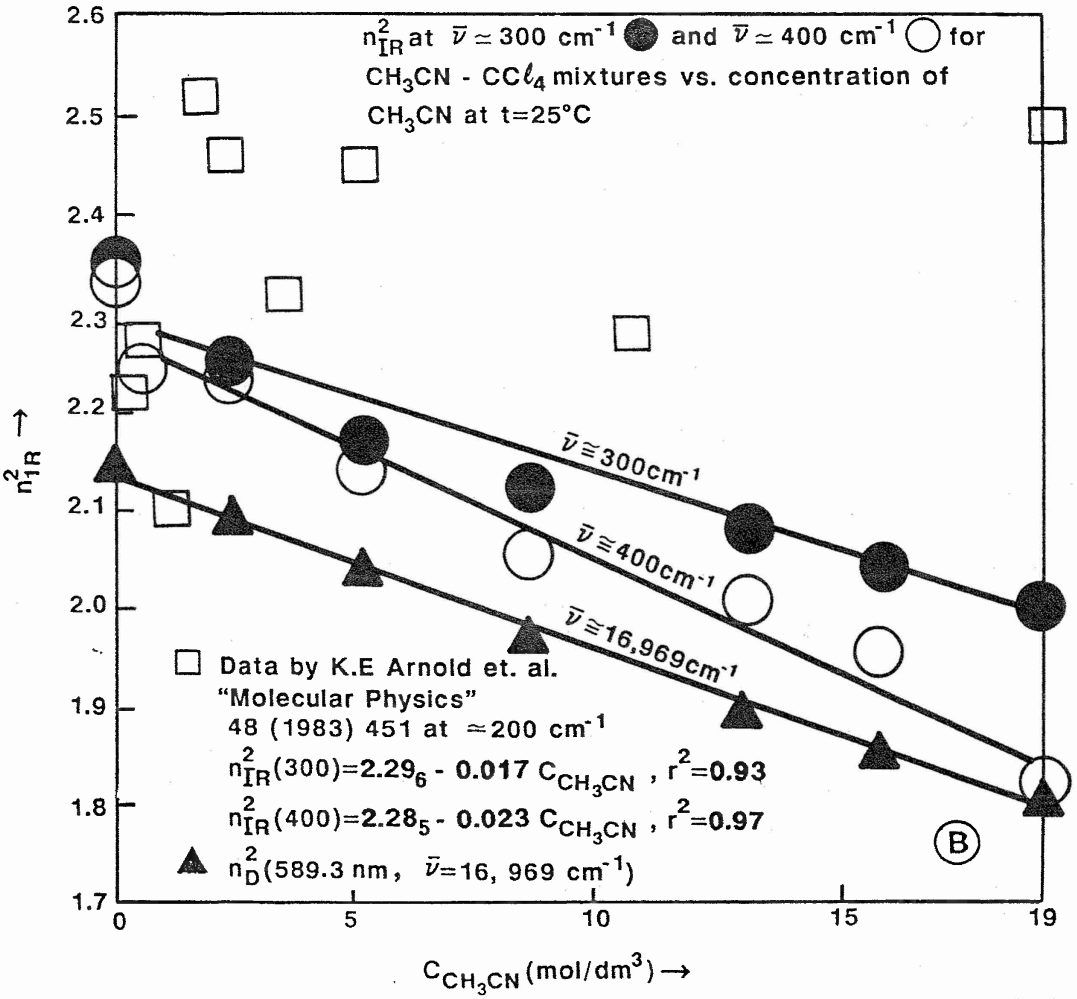
n^2_{IR} at $\bar{\nu} \simeq 300\ cm^{-1}$ ● and $\bar{\nu} \simeq 400\ cm^{-1}$ ○ for
CH_3CN - $CC\ell_4$ mixtures vs. concentration of
CH_3CN at t=25°C
$\bar{\nu} \cong 300 cm^{-1}$
$\bar{\nu} \cong 400 cm^{-1}$
$\bar{\nu} \cong 16{,}969 cm^{-1}$
□ Data by K.E Arnold et. al.
"Molecular Physics"
48 (1983) 451 at ≃200 cm^{-1}
$n^2_{IR}(300) = 2.29_6 - 0.017\ C_{CH_3CN}$, $r^2 = 0.93$
$n^2_{IR}(400) = 2.28_5 - 0.023\ C_{CH_3CN}$, $r^2 = 0.97$
▲ n^2_D(589.3 nm, $\bar{\nu}$=16, 969 cm^{-1})
B
n^2_{1R} →
C_{CH_3CN} (mol/dm³) →

Fig (8)

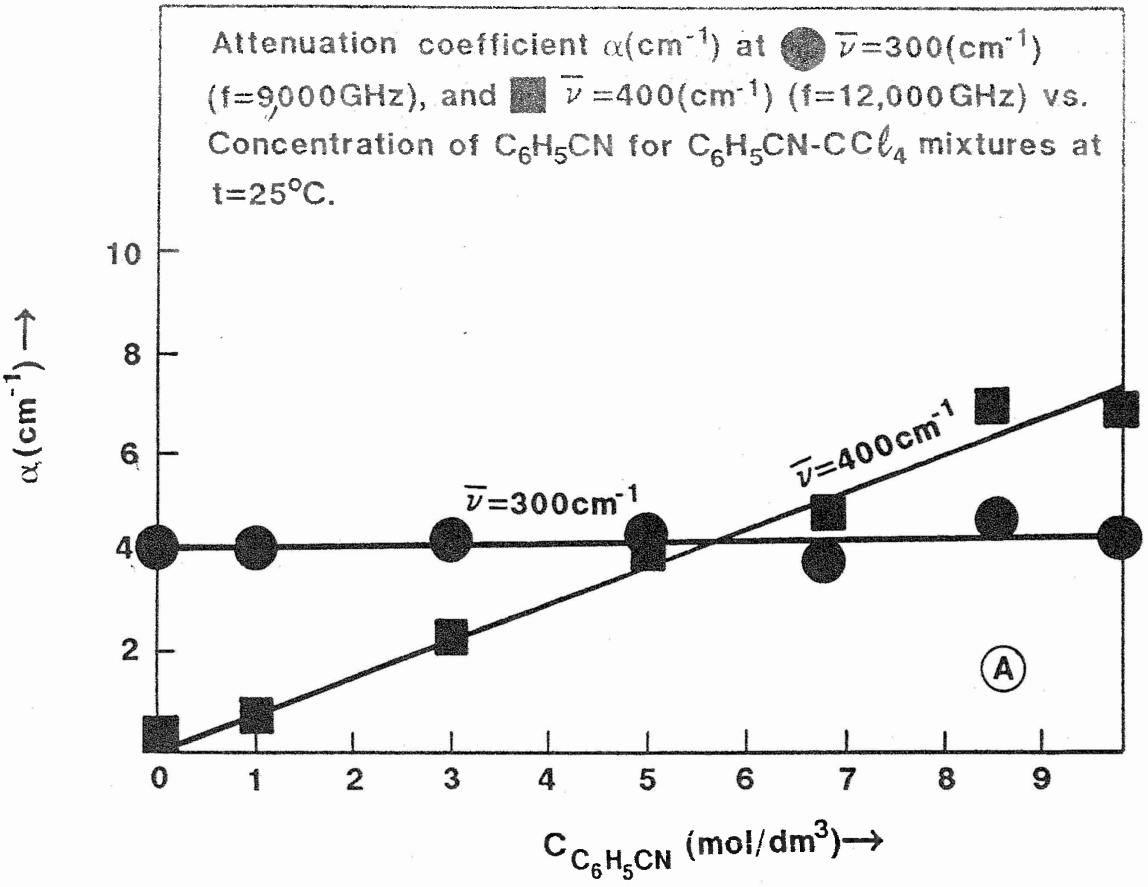
Attenuation coefficient α(cm⁻¹) at ● ν̄=300(cm⁻¹) (f=9,000GHz), and ■ ν̄=400(cm⁻¹) (f=12,000GHz) vs. Concentration of C6H5CN for C6H5CN-CCℓ4 mixtures at t=25°C.
α(cm⁻¹) →
ν̄=300cm⁻¹
ν̄=400cm⁻¹
A
C C6H5CN (mol/dm³)→

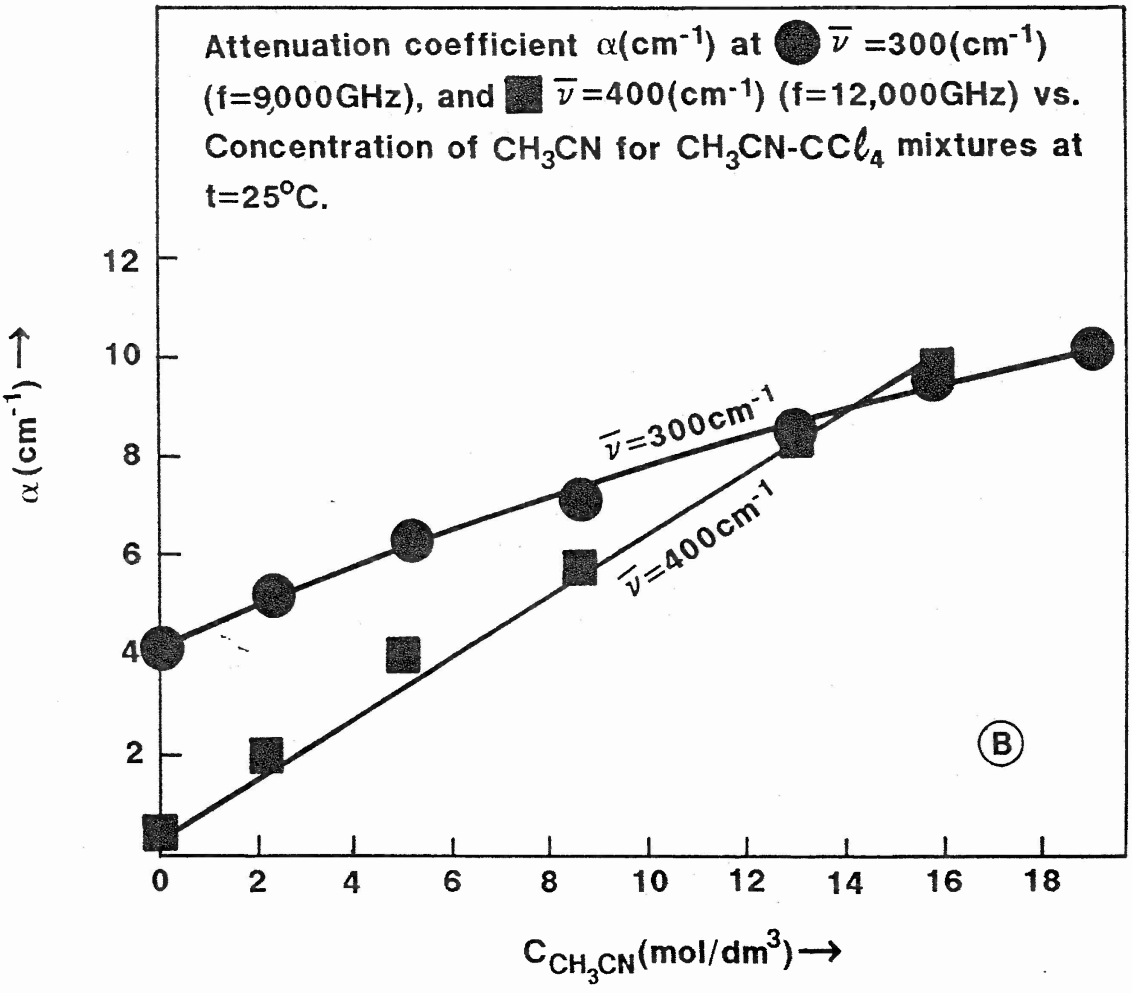
Attenuation coefficient α(cm⁻¹) at ● ν̄ =300(cm⁻¹) (f=9,000GHz), and ■ ν̄=400(cm⁻¹) (f=12,000GHz) vs. Concentration of CH3CN for CH3CN-CCℓ4 mixtures at t=25°C.
α(cm⁻¹) →
ν̄=300cm⁻¹
ν̄=400cm⁻¹
B
C CH3CN(mol/dm³)→

Fig. 9

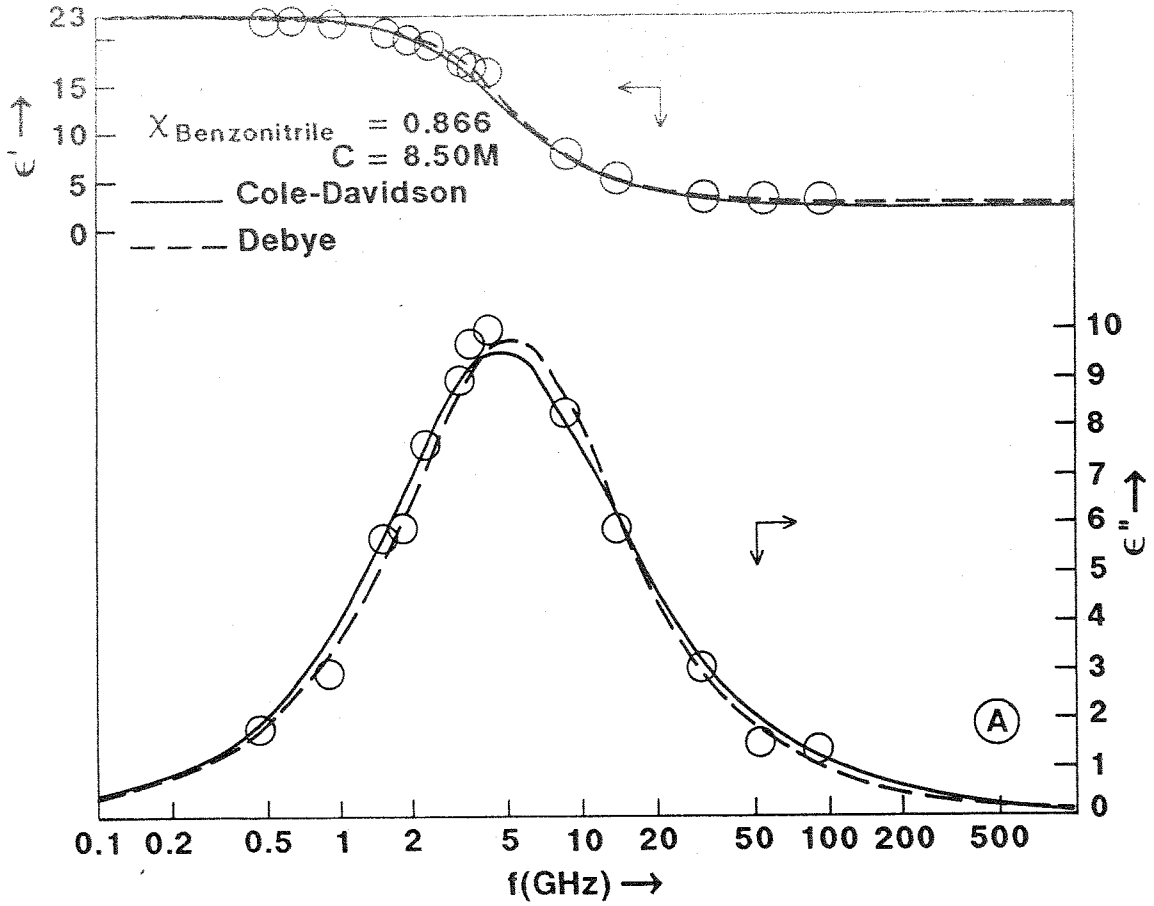
23
15
10
5
0
ε'
X Benzonitrile = 0.866
C = 8.50M
Cole-Davidson
Debye
10
9
8
7
6
5
4
3
2
1
0
ε"
A
0.1 0.2 0.5 1 2 5 10 20 50 100 200 500
f(GHz) →

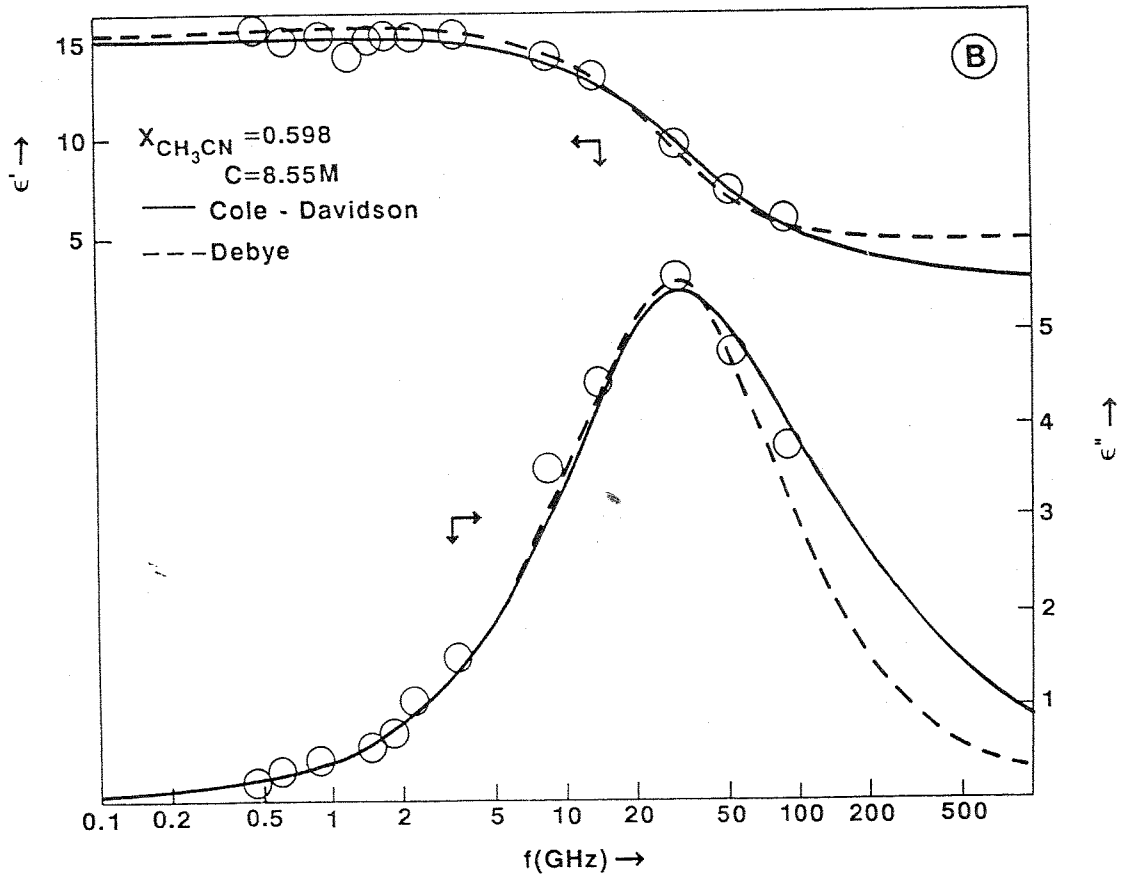
B
15
10
5
ε'
X CH3CN =0.598
C=8.55M
Cole - Davidson
Debye
5
4
3
2
1
ε"
0.1 0.2 0.5 1 2 5 10 20 50 100 200 500
f(GHz) →

Fig. 10

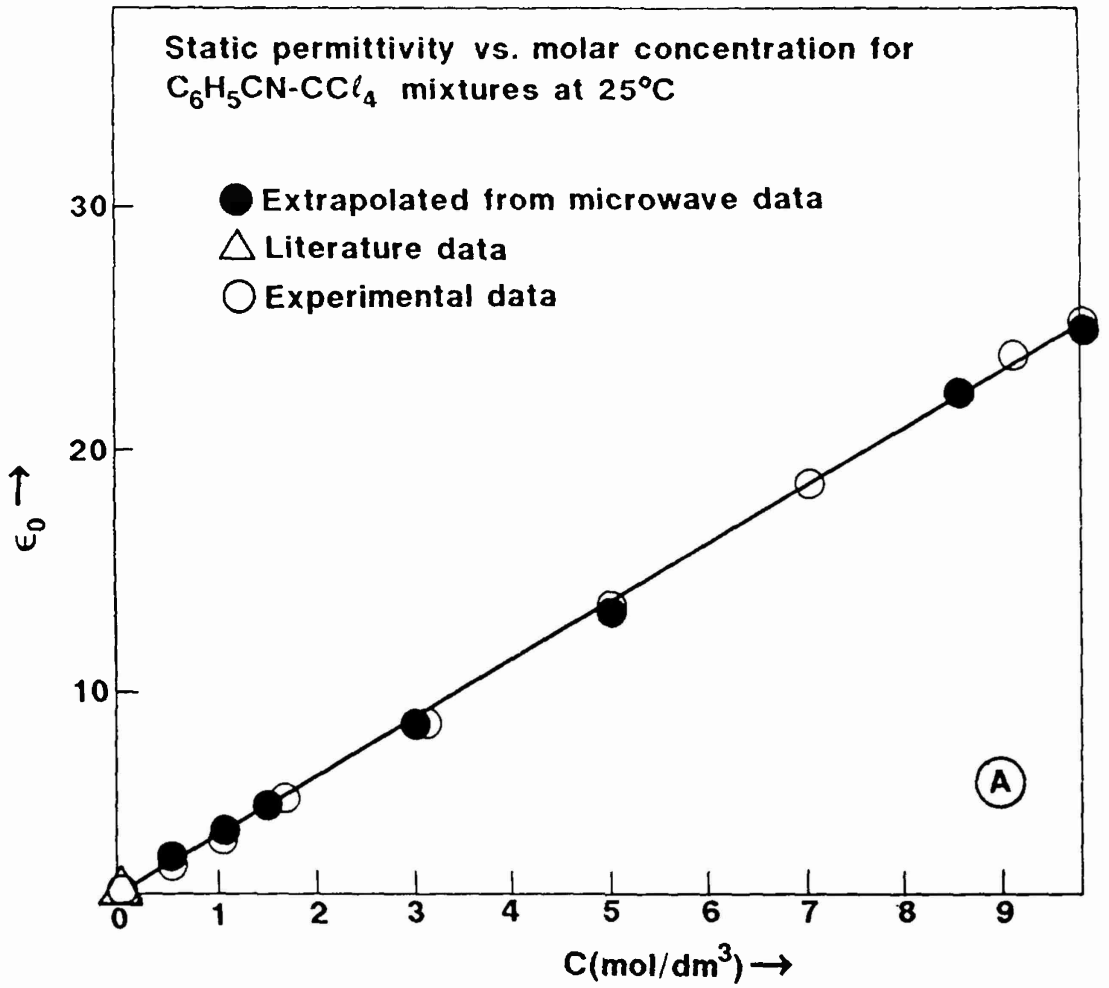
Static permittivity vs. molar concentration for
C_6H_5CN-$CC\ell_4$ mixtures at 25°C
Extrapolated from microwave data
Literature data
Experimental data
ϵ_0
30
20
10
0
1
2
3
4
5
6
7
8
9
A
C(mol/dm^3) →

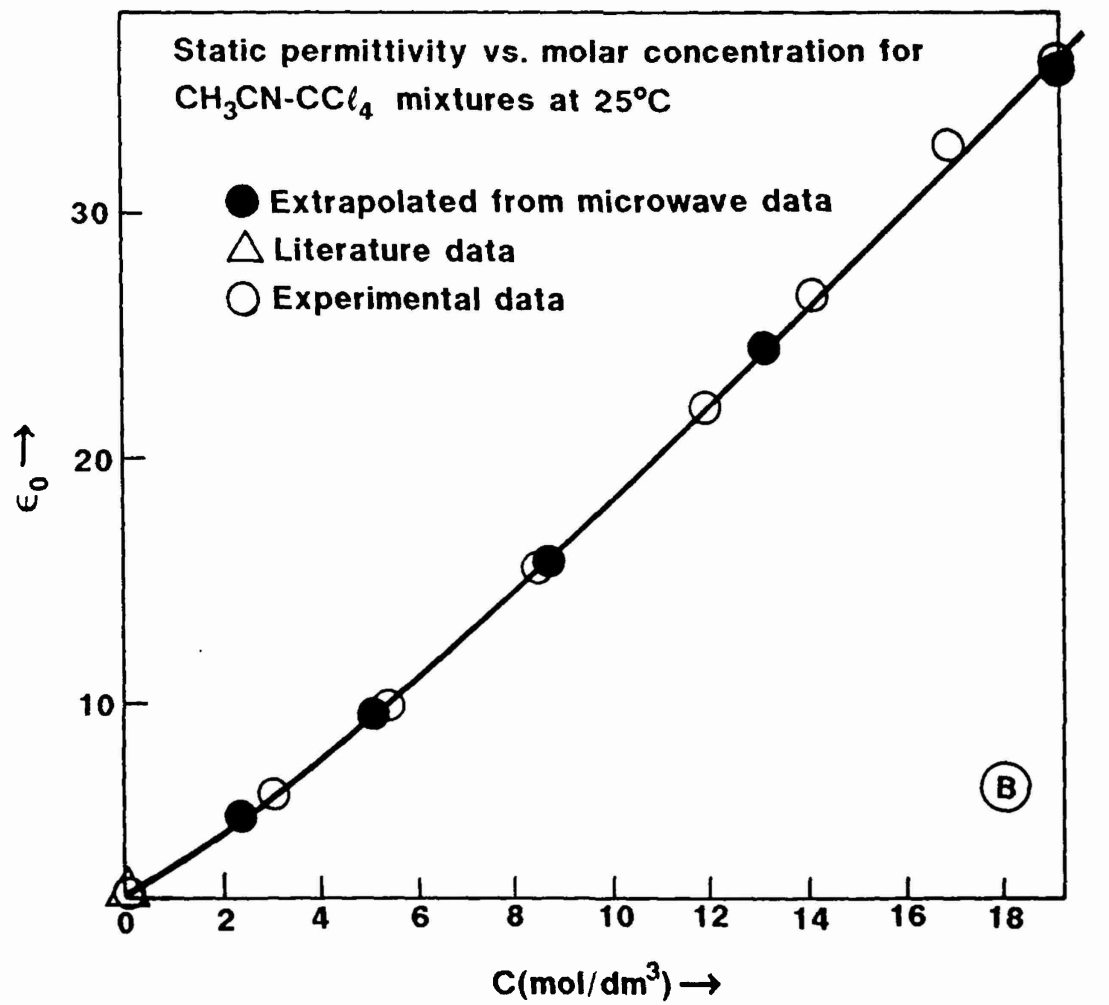
Static permittivity vs. molar concentration for
CH_3CN-$CC\ell_4$ mixtures at 25°C
Extrapolated from microwave data
Literature data
Experimental data
ϵ_0
30
20
10
0
2
4
6
8
10
12
14
16
18
B
C(mol/dm^3) →

Fig. 11

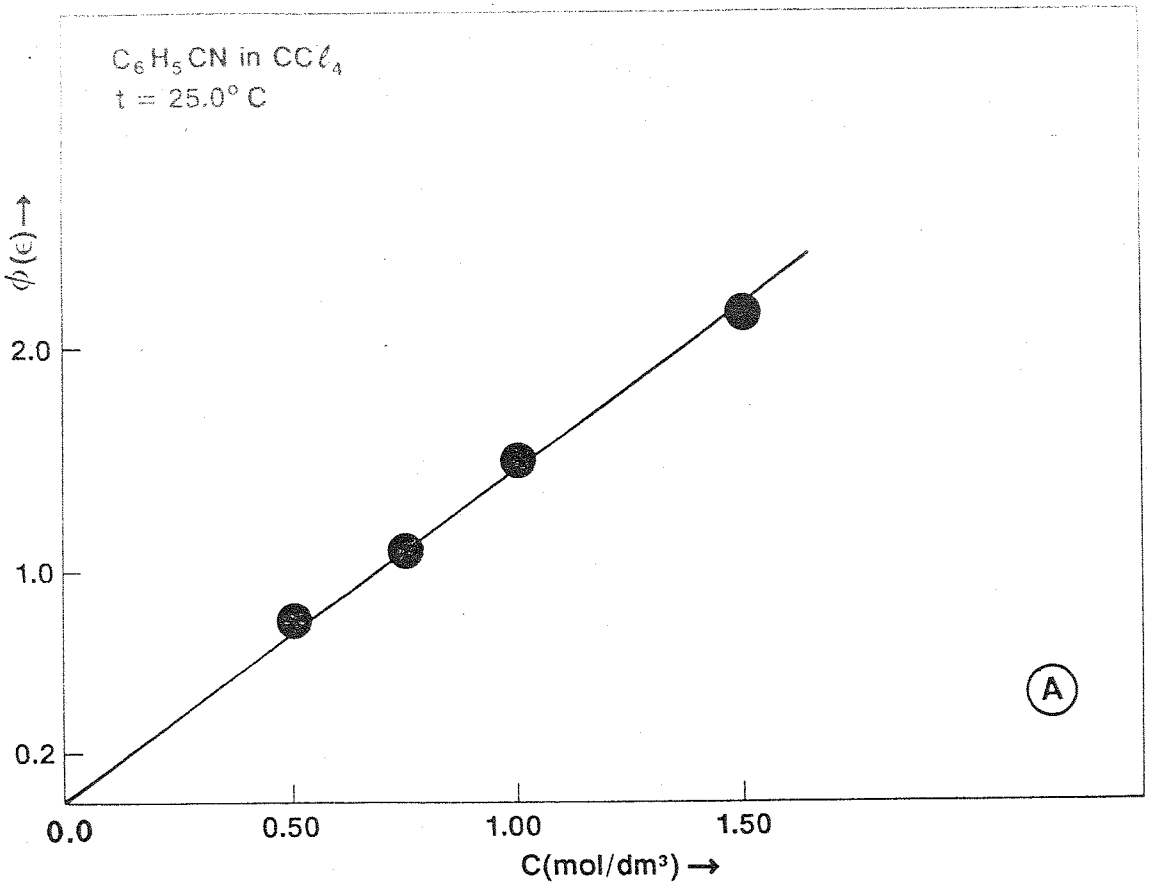

(M)(mol/dm^3) ⟶

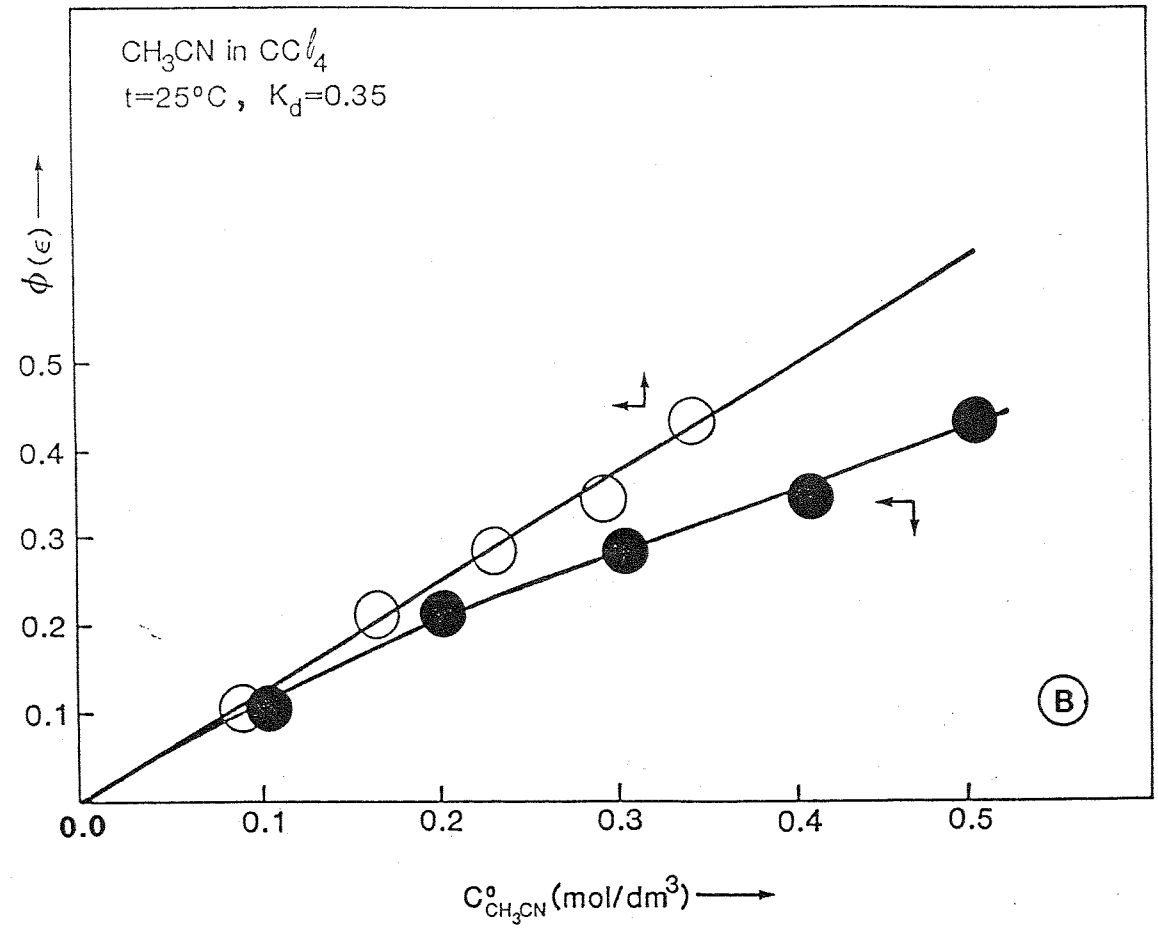

Fig. 12

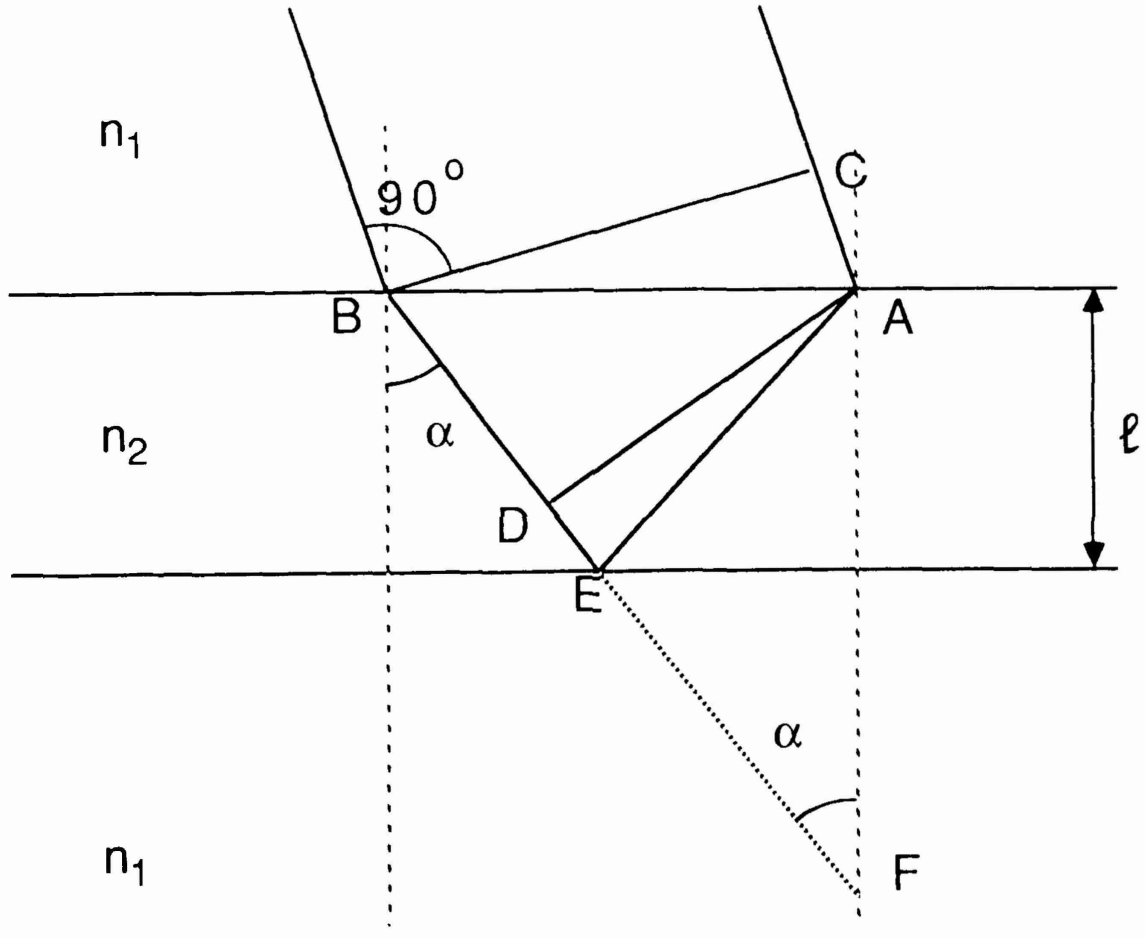
n_1
90°
C
B
A
n_2
α
ℓ
D
E
α
n_1
F